

THESIS FOR THE DEGREE OF DOCTOR OF PHILOSOPHY

**Evaluating Tropical Upper-tropospheric Water in
Climate Models Using Satellite Data**

MARSTON S. JOHNSTON



CHALMERS

Department of Earth and Space Sciences
CHALMERS UNIVERSITY OF TECHNOLOGY
Gothenburg, Sweden 2014

**Evaluating Tropical Upper-tropospheric Water in Climate Models
Using Satellite Data**

MARSTON S. JOHNSTON

ISBN 978-91-7385-958-5

© MARSTON S. JOHNSTON, 2014.

Doktorsavhandlingar vid Chalmers tekniska högskola
Ny serie nr 3640
ISSN: 0346-718X

Department of Earth and Space Sciences
Global Environmental Measurements and Modelling
Chalmers University of Technology
SE - 412 96 Gothenburg, Sweden
Phone + 46 (0)31 772 1000

Cover: Observed and simulated cloud fraction anomalies for land-based deep convective systems in the tropics, $\pm 3^\circ$ latitude, $\pm 10^\circ$ longitude, and ± 48 hours from the center point of peak surface precipitation.

Printed by Chalmers Reproservice
Chalmers University of Technology
Gothenburg, Sweden 2014

To the two stars in my heaven:

Adam Oliver Sebastian Johnston

and

Emma C. Andersson

Evaluating Tropical Upper-tropospheric Water in Climate Models Using Satellite Data

MARSTON S. JOHNSTON

Department of Earth and Space Sciences

Chalmers University of Technology

Abstract

Measuring and simulating moist processes in the tropical upper troposphere are difficult tasks. Humidity in this region of the atmosphere is mainly supplied by deep convection and, problems with simulated convection are known to be a major contributor to uncertainties in climate model projections. Observations within this region of the atmosphere are hampered by the low absolute humidity as well as by the presence of clouds.

This thesis examines the seasonal changes in and the effects tropical deep convection have on upper-tropospheric water, in addition to its effect on outgoing longwave radiation (OLR). Multiple satellite observations are assessed and used to evaluate the climate models EC-Earth, CAM5, and ECHAM6. The data are analysed using two main methods: longterm averages and compositing. Compositing represents an improvement over climatologies because it brings the comparison closer to the processes associated with deep convection. The compositing method is adapted from [Zelinka and Hartmann \[2009\]](#), improved, and applied for the first time to climate models.

Upper-tropospheric humidity (UTH) undergoes large seasonal and regional changes in the tropics. Over land areas, convection is more intense, producing greater amounts of water at higher heights, and having a greater effect on the OLR. Corresponding model simulations capture the large-scale and seasonal changes, however there are significant inconsistencies when compared with the observations, especially over land regions. Simulated mean UTH in areas where DC systems develop are consistently higher than observed over both land and ocean. However, the direct response of UTH to DC systems is found to be similar to the observations. Modeled cloud fractions near the tropopause are tend to be overestimated, whereas ice water content is often too low. The observed OLR can, regionally, differ from the simulated results by as much as 20 W m^{-1} . Moreover, above and around deep convection systems, the local decrease of OLR is throughout underestimated. Further, the models all demonstrate a lack of spatial variability indicated by a diurnal repetition of convection at the same location over land. These results obtained by the composite method reveal details that could not have been obtained using a traditional climatology based comparison.

Keywords: Climate, IWC, Humidity, Clouds, ECHAM6, CAM5, EC-Earth

APPENDED PAPERS

The thesis is based on the following articles:

- Johnston, M. S., Eriksson, P., Eliasson, S., Jones, C. G., Forbes, R. M., and Murtagh, D. P.: The representation of tropical upper tropospheric water in EC Earth V2, *Clim. Dyn.*, 39, 2713-2731, doi:10.1007/s00382-012-1511-0, 2012.
- Johnston, M. S., Eliasson, S., Eriksson, P., Forbes, R. M., Wyser, K. and Zelinka, M. D.: Diagnosing the average spatio-temporal impact of convective systems Part 1: A methodology for evaluating climate models, *Atmos. Chem. Phys.*, 13, 13653-13684, doi:10.5194/acpd-13-13653-2013, 2013.
- Johnston, M. S., Eliasson, S., Eriksson, P., Forbes, R. M., Gettelman, A., Räisänen, P. and Zelinka, M. D.: Diagnosing the average spatio-temporal impact of convective systems – Part 2: A model inter-comparison using satellite data, *Atmos. Chem. Phys.* (submitted).

RELATED PAPERS

Paper in which I have participated but not appended to this thesis:

- P. Eriksson, B. Rydberg, M. Johnston, D. P. Murtagh, H. Struthers, S. Ferrachat, and U. Lohmann. Diurnal variations of humidity and ice water content in the tropical upper troposphere. *Atmos. Chem. Phys.* 10:11519-11533, 2010. DOI 10.5194/acp-10-11519-2010.

CONTENTS

CHAPTER 1 – INTRODUCTION AND OVERVIEW	3
1.1 Earth’s climate system	3
1.2 Carbon dioxide and the greenhouse effect	5
1.3 Climate sensitivity	6
1.4 Observations	8
1.5 General circulation models	8
1.6 Model evaluation	10
1.7 International Panel on Climate Change	11
1.8 Tropical upper troposphere	12
1.9 Objective and structure	13
CHAPTER 2 – TROPICAL CONVECTION	15
2.1 The Tropics	15
2.2 Cumulus convection	17
2.3 Equatorial waves	20
2.4 Deep convection	20
2.5 Tropical circulations	21
CHAPTER 3 – SATELLITE OBSERVATIONS	23
3.1 Satellite observations	23
3.2 Atmospheric infrared sounder	24
3.3 Microwave limb sounder	25
3.4 AMSU-B and MHS	25
3.5 Cloud profiling radar	26
3.6 Cloud profiling lidar	26
3.7 TMPA	27
3.8 CERES	28
3.9 Sampling error	28
CHAPTER 4 – ATMOSPHERIC GENERAL CIRCULATION MODELS	29
4.1 Background	29
4.2 Dynamics and physics	32
4.3 Parameterization	34

4.4	Clouds	35
4.4.1	Cloud microphysics	37
4.4.2	Model uncertainty	38
4.5	Cumulus parameterization	38
CHAPTER 5 – SUMMARY AND OUTLOOK		41
5.1	Longterm mean and composite	42
5.2	Variable definition problem	43
5.3	Appended papers	44
5.3.1	Paper I	44
5.3.2	Paper II	45
5.3.3	Paper III	46
5.4	Outlook	46
REFERENCES		48
PAPER A		55
PAPER B		73
PAPER C		91

ACKNOWLEDGMENTS



This work is in collaboration with, and partially funded by, the Rossby Centre, Department of Research and Development, Swedish Meteorological and Hydrological Institute (SMHI).

I would like to express my gratitude to my colleagues at Global Environmental Measurement and Modelling group and the Rossby Centre at SMHI for their support. Special thanks to Colin Jones, Klaus Wyser, Martin Ewaldsson for their extra support to make this thesis a reality. Special thanks is also reserved for my advisor, Patrick Eriksson, it has not always been an easy road, but much of this work would not be possible without your ideas and help.

CHAPTER 1

Introduction and Overview

This chapter attempts to give a brief overview and some history of the current concern for the planet's climate system. This is an enormously broad and complex topic and cannot be fully addressed here. The following sections highlight some main points and milestones in climate research as they pertain to this thesis. Ultimately, I try to highlight the connection between observations and simulation of the climate systems and the need to improve climate models, all in an effort to better understand the legacy of the Anthropocene¹.

1.1 Earth's climate system

When considering the climate of the Earth, many factors come into play - both external and internal to the planet. External factors governing the climate include the energy provided by the sun, which is one of the basic factors of planetary climate. Our proximity to the sun largely determines the amount of incoming radiation, which falls unequally on the planet as a function of latitude. Changes in the incoming solar radiation depend on changes in the solar cycle as well as changes in the planets orbital properties. These changes occur at times scales that ranges from a decade to many thousands of years.

The different systems on the planet, mainly the ocean, land, ice, vegetation, and the atmosphere react to the incoming radiation and interact with each other to redistribute the differential solar heating. Therefore, the climate of the Earth is described as a system of interconnected sub-systems with feedbacks that can amplify or dampen the effect of changes in the incoming

¹An informal geologic chronological term that marks the evidence and extent of human impact on the Earth's ecosystems.

radiation. This is an example of internal forces controlling the global climate. For millennia, the redistribution of the incoming solar energy has served to balance planetary heat loss with the heat gain and has kept the global temperature at around 288 K.

The climate of a particular region is generally defined as the statistics of the weather over a time frame of about 30 years. It can be described as, for example, the expected average temperature, rainfall, humidity, or cloudiness depending on the time of year. Around the planet, the climate close to the surface ranges from cold near the poles, temperate in the middle latitudes, and warm in the tropics. Therefore, the climate of a region depends largely on its latitude. Other factors also control the climate of a region, these include its height above sea level, its proximity to water and the properties of that water body, and orography, to name a few.

The evolution of the climate system is governed by physical principles that, if they are well known and we know the initial state of the climate, it would be possible to produce a climate projection that has little or no statistical uncertainty. But the factors that govern the climate's evolution are not well known and we cannot measure all the climate's systems in full detail. Nevertheless, the climate does lend itself to statistical descriptions. Nonlinear processes in the climate system act to amplify disturbances in such a manner that predictability is lost after a certain time. However, there are dissipative processes in the climate system, such as surface friction, that acts to keep it within certain predictable boundaries.

Changes in the climate that last for decades and beyond are considered significant and can originate from within the climate system and/or from external forces. The planet's climate has always changed. This has been verified by geological records of past climate states². Changes in past climate have shown that any change in the energy balance between the incoming and outgoing radiation will initiate a change. Examination of past climate change has verified climate's sensitivity to changes in the global atmospheric CO₂ concentrations. Over the last century changes in the climate have occurred more rapidly than before. The burning of fossil fuels increases the atmospheric concentration of CO₂ together with deforestation and other changes in land use have been identified as some examples of human activities changing internal factors that govern the planet's climate and leading to an unequivocal global warming. In order to understand the ongoing changes to the climate system, observations and simulations of past and future climates are studied.

Future climate projections designed to assess the impact of anthropogenic

²http://www.eo.ucar.edu/basics/cc_3.html

effect on the climate system are not without a number of uncertainties. There are three primary causes to such uncertainties. The first is the presence of incomplete knowledge and limited understanding of, for example, climate physics, which limit the accuracy of climate models. The second cause of uncertainties arises from the natural variability of the climate system, both simulated and observed, and has an inherent unpredictability that can sometimes mask the effects of climate change. The final uncertainty stems from unknown future of socio-economic trends. This thesis falls within the realm of the first uncertainty source.

1.2 Carbon dioxide and the greenhouse effect

Observations of the Earth and its climate system have been ongoing for millennia, but collecting and analyzing observational data did not become systematic until the early 20th century. Over the next 100 years, Earth observations have evolved from ground-based sensors, human observers, and simple cameras to high-altitude airborne crafts and later on to its next natural step, space-borne satellites. To date, the planet's hydrosphere, biosphere, atmosphere, and lithosphere all have dedicated observational platforms that include measurements of atmospheric gaseous species such as CO₂, O₃, H₂O, land use, ice thickness, and sea surface temperature.

In the late 19th century it was not yet known what governed the onset and termination of the planet's various ice ages. The concept of *green house effect*³ was put forth as an explanation as to why the Earth is so warm at the surface ($\sim 15^\circ\text{C}$) given its distance from the sun⁴. Building on this theory, Svante Arrhenius⁵, in 1896, theorized that changes in the concentration CO₂, a well-mixed atmospheric gas, could affect the global mean temperature. His theory implied a proportional relationship between this trace gas and the global mean temperature via a formulation that is still used today: $\Delta F = \alpha \ln(C/C_0)$, where ΔF is the radiative forcing, in W m^{-2} , C is the global atmospheric CO₂ concentration in parts per million volume (ppmv), C_0 is a baseline reference for global atmospheric CO₂ concentration (typically a pre-industrial concentration value of 280 ppmv), and α is a constant between five and seven [Myhre et al., 1998].

Arrhenius formulation assumes radiative equilibrium between the incoming solar radiation and the outgoing longwave radiation [Manabe, 1997]. He

³http://en.wikipedia.org/wiki/Greenhouse_effect

⁴This region of space within which the Earth orbits is commonly known as the *Goldilocks* or habitable zone.

⁵http://en.wikipedia.org/wiki/Svante_Arrhenius

predicted that a doubling of CO₂ concentrations could change the global mean temperature by $\sim 5^\circ\text{C}$. While this value would be adjusted for feedback processes, Arrhenius did not take into account other effects from, for example, clouds or convection. Nevertheless, with this simplified example model of the climate system, Arrhenius considered that anthropogenic emission of CO₂ would change the planet over a period of several millennium and prevent a new ice age, an overall positive view, then, of the anthropogenic CO₂ effect.

Up until the mid 20th century, Arrhenius theory was not widely accepted and neither was it without controversy. Some argued that the atmosphere was already saturated with CO₂, while others argued that ocean would absorb all anthropogenic emission. The former argument was based on observation of CO₂ taken within the planetary boundary layer and very close to its source. The latter argument was based on estimates of global emissions, as there were no global measurement of atmospheric CO₂ until the mid 1950s. The need for global atmospheric observations is therefore critical in order to understand the concept of greenhouse gases and the current and projected effect on the climate system with any change in their concentrations.

1.3 Climate sensitivity

In order to understand the response of the global climate system to forcings both internal and external, we need to determine the system's sensitivity to such forcings. Climate sensitivity, expressed in $^\circ\text{C}$, is a fundamental aspect of the system and is normally determined with regards to the change in the planet's radiation balance brought about by a doubling of atmospheric CO₂. In atmosphere-ocean climate models, climate sensitivity is function of the synergy between many aspects of the model, for example, its physics. However, simpler energy-balance models use a climate sensitivity that is defined differently. In this case, climate sensitivity, λ expressed in $^\circ\text{C}/(\text{W}/\text{m}^2)$, translates a particular radiative forcing, ΔF , into a change in the global surface temperature, ΔT , after equilibrium in the climate systems has been reached ($\Delta T = \lambda \times \Delta F$).

Quantifying the planet's climate sensitivity to a doubling of CO₂ has proven to be a difficult task. Climate sensitivity calculated using observations from recent past, going back millennia, and using model-simulated data have been able to establish a lower limit with good confidence. Uncertainties in the climate forcing and the physics of the system's response make establishing an upper bound difficult and create extreme cases and outliers [Knutti and Hegerl, 2008, Fig. 3]. Climate sensitivity obtained from an ensemble of simulated climate projections is called effective climate sensitivity as models do not

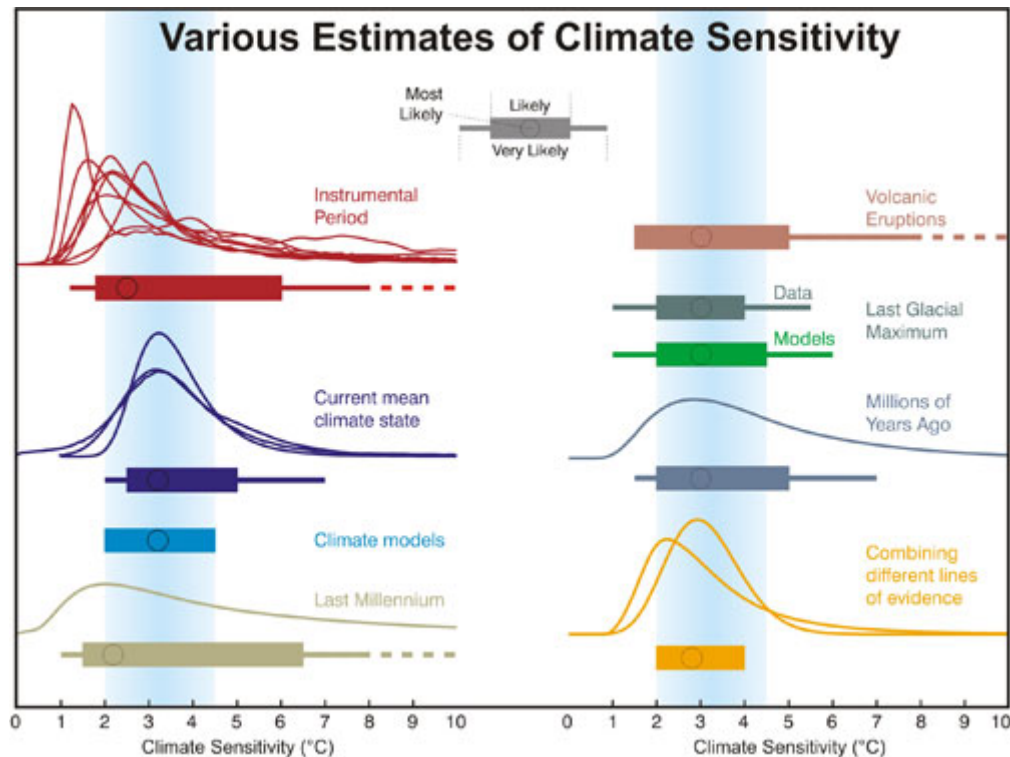


Figure 1.1: *Climate sensitivity from several sources. The most likely values are depicted by circles, likely values are given bars (> 66% probability), and very likely are shown as lines (> 90% probability). Dashed lines indicate no robust constraint on an upper bound. Distributions are truncated in the range 0–10 K. The IPCC likely range and most likely value are indicated by the vertical grey bar and black line, respectively. Source: original from Knutti and Hegerl [2008] but this adapted example can be found at <http://www.skepticalscience.com/climate-sensitivity-advanced.htm>.*

run long enough to reach equilibrium state. Figure 1.1 illustrates the various climate sensitivity values obtained from models and observations as well as an estimate derived from a combination of the different lines of evidence. While the range for the climate sensitivity discussed is simply based on forcing caused by changes in CO_2 concentrations, it nevertheless gives us an idea of what to expect for changes in the global temperature caused by other types of forcing.

1.4 Observations

Observations are critical in the understanding of the climate system. Although ground-based observations of atmospheric CO₂ have existed since the late 19th century, they were not very precise nor were they reliable. It was not until Charles Keeling⁶ established a monitoring station at the Mauna Loa Observatory in 1956, that the world's first benchmark for global atmospheric CO₂ concentration was created. Since then, proxy observations have confirmed that the planet's climate is ever changing and ice core measurements of atmospheric CO₂ concentrations over the last 200 years has risen at rates not seen during the last $\sim 500\,000$ years⁷. At the rate of approximately 2 ppm per year (2013)⁸, this atmospheric trace gas has risen from about 280 ppm about 100 years ago [Keeling, 1997] to roughly 395 ppm as of Dec 2013⁹. Fig. 1.2 shows the timeseries of CO₂ concentrations for the last half century. The rate of increase is highly correlated to the increase in human energy consumption and population increase. The Mauna Loa Observatory is a single ground station, and, in order to monitor the planet, the next logical step was space-borne satellites. Remote sensing observations of the planet's climate system came of age with the advent of satellites, but it was not until the mid 1990s that satellites dedicated to monitoring the Earth's climate were launched. Measurements of atmospheric infrared emission, microwave emission, reflected ultra-violet, and visible light are all part of the current global observing system. While observations tell us what is going on in the climate system, they are only snapshots in time. What is desired is a forecast of the future climate, and general circulation (climate) models, largely because they can simulate feedback processes, are the best tool for quantifying changes to come.

1.5 General circulation models

The idea of a numerical model was first postulated by Bjerknes et al. [1904] based on the assumptions that subsequent atmospheric states develop from a proceeding one in a manner that is governed by physical laws. If the interaction between the systems involved is sufficiently well known and their initial states can be ascertained with enough accuracy, then a future atmospheric state can be simulated. But it was not until the 1950's, when computers were

⁶http://en.wikipedia.org/wiki/Charles_Keeling

⁷https://www.ipcc.ch/publications_and_data/ar4/wg1/en/tssts-2-1-1.html

⁸<http://www.esrl.noaa.gov/gmd/ccgg/trends/>

⁹<http://www.esrl.noaa.gov/gmd/ccgg/trends/global.html>

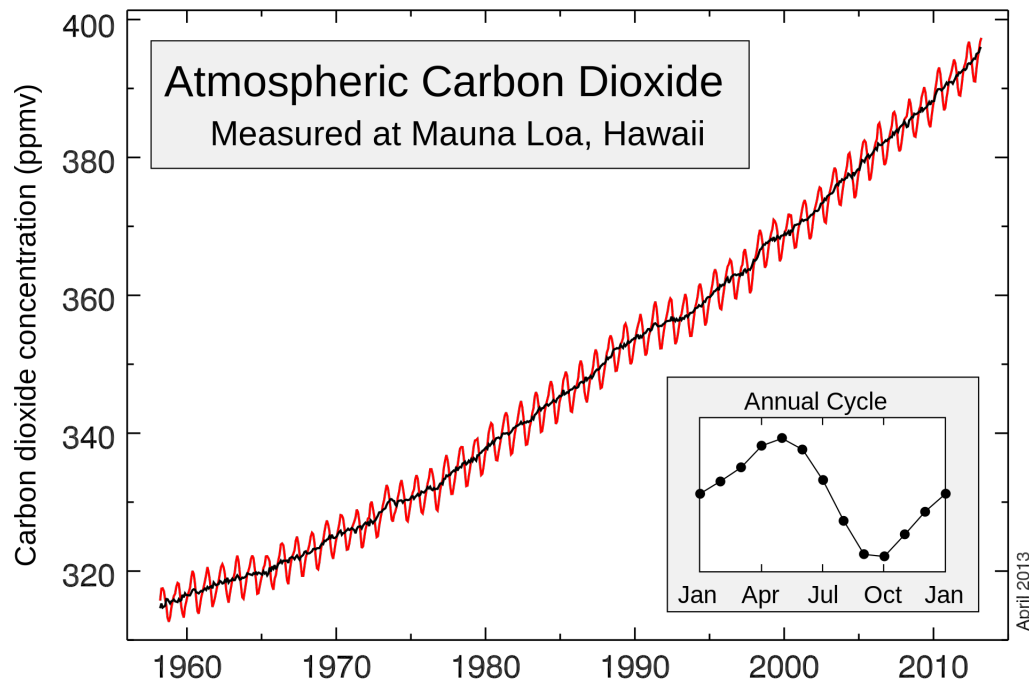


Figure 1.2: Timeseries “Keeling curve” of global atmospheric CO₂ from 1956 to April 2013. Superimposed on the figure, bottom right, is the annual cycle. Source: http://en.wikipedia.org/wiki/Keeling_Curve.

used to solve numerically the equations governing the atmosphere, that the first forecast was made. Climate models evolved out of numerical weather predictions models and are able to run for hundreds of years. In order to represent the climate, each sub-component of the climate system need to be simulated. Some of the first climate models could not fully represent the radiative balance between the sun and the Earth because convection was not represented [Manabe and Strickler, 1964; Manabe and Wetherald, 1967]. Over the years, and in step with advancements in computer processing and observations, more sub-components have been added to climate model. Today, there can be an atmospheric, ocean, land-surface, sea ice, vegetation, and chemistry component present in a climate model. One advantage of complex models is that they are able to simulate the feedbacks found in the climate system, which is necessary to determine the climate sensitivity. However, as the complexity of climate models increases it has the undesired effect of making them harder to evaluate.

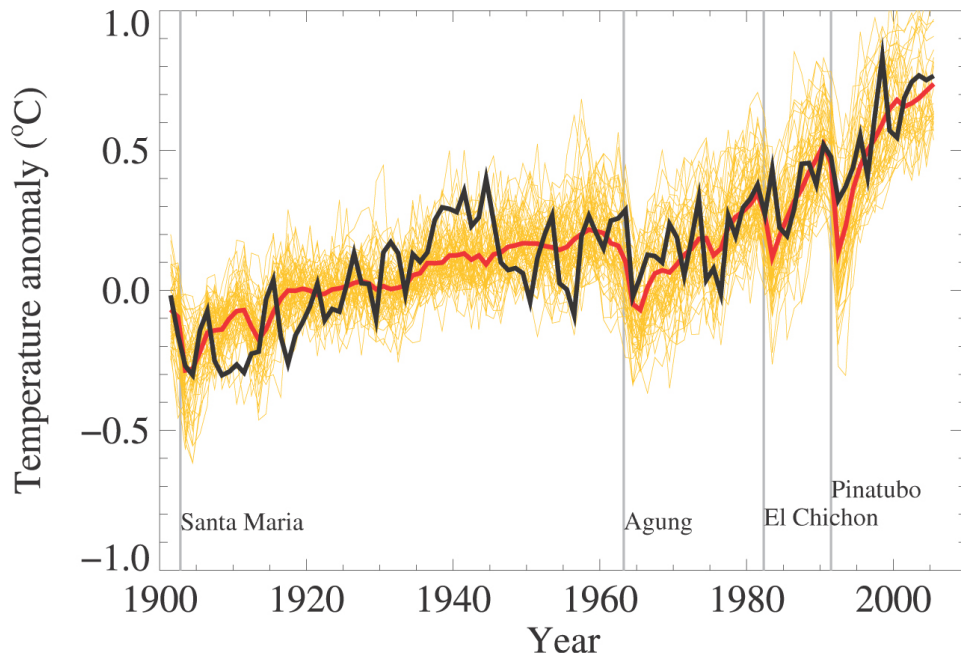


Figure 1.3: Mean global near-surface temperature for the past century. Observations (black) are plotted together with 58 simulations (yellow) produced by 14 different climate models. The mean of all these runs is also shown (thick red line). Vertical grey lines indicate the timing of major volcanic eruptions. Source: IPCC Fourth Assessment Report.

1.6 Model evaluation

GCMs are able to capture observed features of past and recent climate changes. Together with available observations as constraints, the climate system sensitivity can be better assessed, which enables us to better understand the response of the climate system to external and/or internal forcing. However, we are still unable to significantly improve on Svante Arrhenius prediction of $\approx 5\text{ K}$ increase in the global mean temperature for a doubling in the global atmospheric CO_2 concentration. It is estimated that if CO_2 concentrations were to reach 580 ppmv, the planet will likely see a temperature rise $\sim 3^\circ\text{C}$ (see Fig. 1.1), but this improvement of the $\sim 5^\circ\text{C}$ advanced by Arrhenius is not without a degree of statistical uncertainty, extremes, and outliers.

Some tests that are performed on climate models are:

1. Simulations for the recent past 50 – 150 years, where the mean state, climate changes, and variability at various timescales, for example, are examined.

2. Paleoclimate modelling, where the last glacial maximum and millenium are exmined.
3. Idealized test such as a doubling of global atmospheric CO₂ concentra-tions are exmined

Figure 1.3 illustrates the ability of models to simulate past climate. However, a climate model's performance cannot be easily ascertained when projecting, e.g., 100 years into the future. Instead, confidence is gained by judging the accuracy of recent and past climate scenarios - but this is insufficient. In order to increase model fidelity, reduce the statistical uncertainty in future climate projections, and improve the estimates of climate sensitivity, models need to undergo comprehensive evaluations on identified areas of weakness. By subjecting models to rigorous tests on multiple levels, errors can be identified and corrected [Randall et al., 2007]. Models need to subjected to more tests that evaluate the inner workings.

Today, GCMs are evaluated in many more ways; in particular, components can be compared (so called component level), or via system level where the model output is compared. Another more useful method involves ensembles of output from a number of models in order to study the lower and upper bounds of the possible climate projections in response to a specific forcing. System level evaluations can be carried out using a *model to retrieval* comparison or by simulated satellite radiances with the aid of a satellite simulator such as Cloud Feedback Model Intercomparison Project (CFMIP) Observation Simulator Package (COSP) [Bodas-Salcedo et al., 2011]. Both *model to retrieval* and *simulated radiance* methods have advantages and disadvantages when trying to bring both the model and the satellite definitions as close to each other as possible. However, when studying cloud feedback processes, a satellite simulator is often employed. Special focus is often given to a region, or regions, of any of the climate's sub-system previously identified as problematic as well as any particular model output. One such region is the upper troposphere where observations are limited, and an example of a variable is the representation of clouds, which is considered one of the largest source of model uncertainty [Randall et al., 2003].

1.7 International Panel on Climate Change

Global warming is unequivocal, and the view of most scientist today is that the effects of a rapid increase atmospheric CO₂ concentrations, to levels of 400 ppm and beyond, are not positive. For example, the melting of the polar ice caps will lead to a change in the planet's albedo, the oceans are becoming

more acidic due the absorption of high amounts of CO₂, are effects that are threatening much of the life on the planet. In order to understand the effects of increased concentrations of greenhouse gases, one needs to understand the processes involved and how they affect each other. This tantamount to understanding how the global carbon cycle functions, and it follows that only then can we fully understand how anthropogenic changes in CO₂ will affect the future climate. Climate change on such a scale is not a simple task and so the United Nation created the Intergovernmental Panel on Climate Change (IPCC) for the assessment of climate change. Every few years the IPCC publishes a report that updates the current science and conclusions regarding global warming. A part of the IPCC report consists of the results of a Coupled Model Intercomparison Project (CMIP) within which many models from many research centers around the world compare standardized outputs. Coupled to the CMIP data is the Atmospheric Model Intercomparison Project (AMIP), which is a dataset where only the atmospheric component of a GCM is run, using boundary conditions. Data from the AMIP archive is meant only for scientific evaluation of models and provides freely data from many modelling centers around the world.

1.8 Tropical upper troposphere

The importance of CO₂ has been discussed so far, but another important greenhouse gas is water vapor. Water vapor is the most dominant natural greenhouse gas and is responsible for the largest positive feedback in the climate systems [Soden and Held, 2006]. Any change in this atmospheric constituent is important for future climate projections. In the free troposphere¹⁰, CO₂ is a well mixed gas, but water vapor varies greatly and decreases with height as the temperature decreases, according to the Clausius-Clapeyron equation. In the upper troposphere, the cold temperatures keep the water vapor at low concentration levels, but as the planet warms, the water vapor content of the troposphere will increase. The absorptivity of water vapor is proportional to the logarithm of its concentration [Soden et al., 2005] therefore, in regions of the troposphere with low concentrations, fractional increases can give rise to large absorption of radiation, which can cause a significant feedback into the climate system [Solomon et al., 2007, Chap. 8 Box 8.1]. This underpins the necessity for understanding the observed moist processes in the upper troposphere and their projected changes.

¹⁰The region of the troposphere above roughly 2 km from the surface.

1.9 Objective and structure

The objective of the thesis is to summarize and give an overview of the work underpinning three appended papers that are concerned with the following:

1. Assessing measurements of upper-tropospheric water and its representation in the climate model EC-Earth
2. Diagnosing the spatio-temporal effect of deep convection on upper-tropospheric moist processes using a composite technique and demonstrating the technique's viability to do the same in the climate model EC-Earth version 2
3. Expanding the objective in item 2 to include an inter-comparison between EC-Earth version 3, CAM5, and ECHAM6

Chapter 1 gives some background information on the work presented in this thesis. Chapter 2 provides a brief overview of tropical convection. Chapter 3 provides general review of satellite remote sensing and observation systems employed. Chapter 4 gives overview of the current state of climate models and finally, Chapter 5 presents a summary and outlook.

CHAPTER 2

Tropical Convection

This chapter gives a brief description of the tropics and one of its most important weather phenomenon: moist convection. The discussion on convection is later limited to deep convection, which is the focus of this thesis. Much of this chapter is based on the books [Smith \[1997\]](#) and [Holton \[1994\]](#).

2.1 The Tropics

The astronomical definition of the tropics is the area between $\pm 23.5^\circ$ latitude, but in this thesis, it is defined using the more meteorologically meaningful definition of $\pm 30^\circ$ latitude. The tropics are important in many ways, and one major aspect is the amount of incoming solar radiation. [Figure 2.1](#) shows the annual mean net longwave and net shortwave radiation per latitude. From the figure it is clear that the tropics get a surplus of energy.

This excess energy is stored in the atmosphere and ocean before being transported towards the poles. The transport of energy polewards within the oceans and atmosphere teleconnects the tropics to the remainder of the planet and gives this region special importance. Dynamically speaking, the main difference between the tropics and the rest of the planet is the magnitude of the *Coriolis* parameter: $f = 2\Omega \sin \theta$, where Ω is the rotation speed of the planet and θ is the latitude. In the tropics the Coriolis parameter is small.

In the tropics many weather phenomena have a diurnal cycle of about 24 hours and occur on local- to meso-scale (~ 5 km and ~ 100 km). A particular important region of tropical disturbances is a zonally (east to west) oriented band called the InterTropical Convergence Zone (ITCZ). The ITCZ forms where the northeast and southeast trade winds converge. Over land regions, the seasonal movement of this band follows the sun, but over the oceans, this

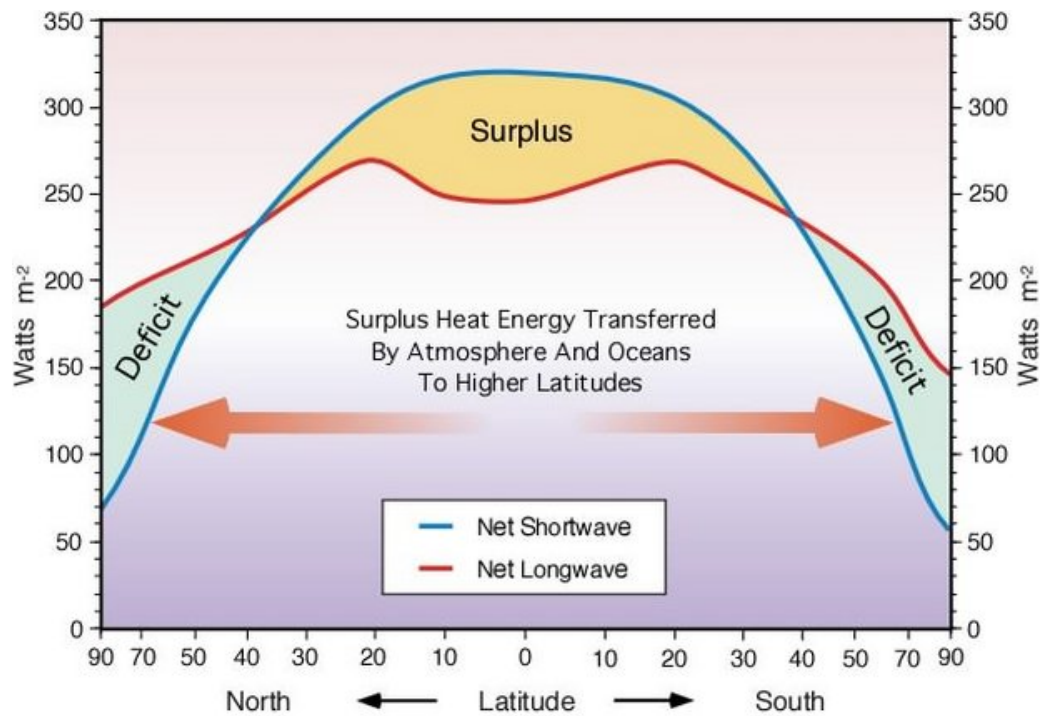


Figure 2.1: Annual mean net outgoing longwave radiation (red) and net incoming shortwave radiation (blue) per latitude. Source: <http://www.physicalgeography.net/fundamentals/7j.html>

movement is smaller. In Figure 2.2 the ITCZ becomes visible by looking at a longterm mean of precipitation in the region. The top plot shows the observed mean (1980 – 1999), and the bottom plot shows a simulated representation. The figure clearly shows concentrations of precipitation over the western Pacific and Indian ocean south of India.

The energy source for tropical disturbances is in the form of convection, which is the primary weather generating process in the region and mainly concentrated along the ITCZ. Observations and experiments have shown that energy balance in the tropics is achieved with the aid of convection, hence the tropics is in radiative-convective balance, more so than the mid-latitudes or the poles. Therefore, more than any other place on the planet, convection is important in the tropics [Manabe and Strickler, 1964; Manabe and Wetherald, 1967].

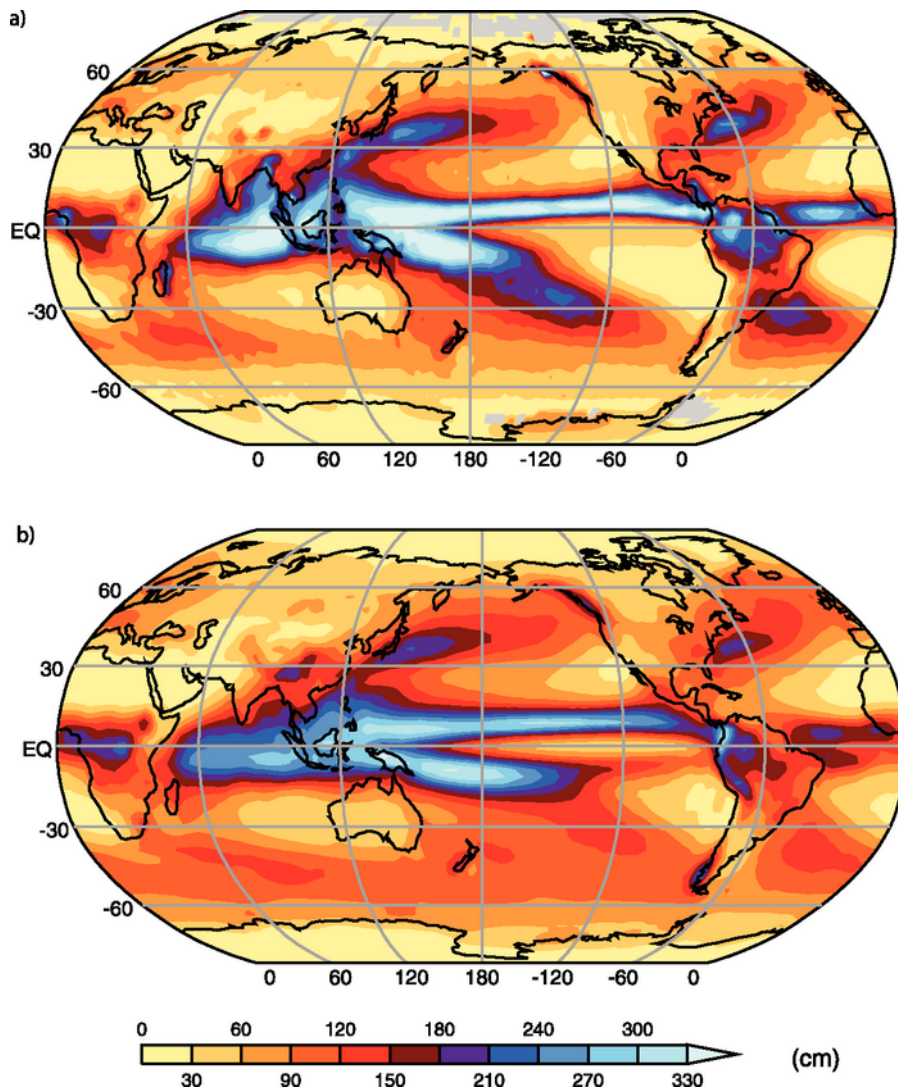


Figure 2.2: *Observed and simulated mean annual precipitation (1980 to 1999). Observed (a) and simulated (b), based on the multi-model mean. Source: IPCC AR4*

2.2 Cumulus convection

In the tropics cumulus, or moist, convection is the conduit by which water, heat and momentum are transported from the planetary boundary layer vertically to the tropopause – and even the lower stratosphere. However, only a small portion of the total convective activity reaches the tropopause. Convection plays a fundamental role in the atmospheric energy cycle, the water cycle, and the global climate. The evolution of convection basically follows three

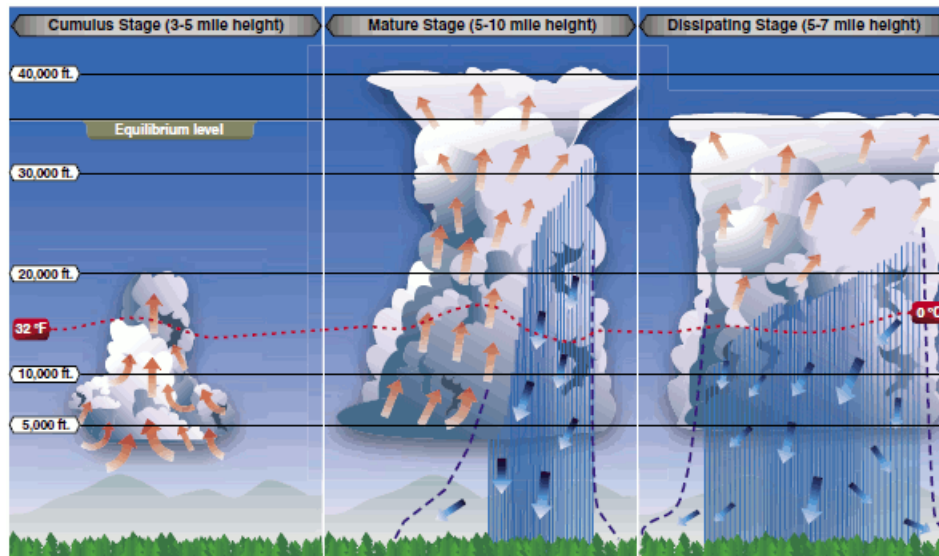


Figure 2.3: The three typical stages in the life cycle of convection. Source: <http://www.aero-mechanics.com/wp-content/uploads/2011/10/11-23.gif>.

stages: cumulus, mature, and dissipating. As cumulus clouds grow, they pass through several known phases of development with special nomenclatures to indicate these new cloud forms. From the initial small cumulus cloud one sees on a fair weather day, these innocuous clouds then grow into tall *towering cumulus* and then *cumulus congestus*, achieving greater vertical penetration with each phase. In the final phase, cumulus clouds are called *cumulonimbus* with a signature fanning out of it cirrus shield to form an anvil-like top. Figure 2.3 illustrates the three major stages of cumulus development. In the initial stage (cumulus stage) convection occupies a very small spatial domain, $\sim 1 \text{ km}^2$, and can grow and organize into aggregations with a coverage of $\sim 1000 \text{ km}^2$. The mature stage follows the cumulus stage, where convection reaches its maximum vertical height and precipitation begins. Finally, there is the dissipation stage where mainly precipitation occurs and the vertical velocities are almost totally negative. The maximum precipitation rates occur in the dissipation stage. The duration of convection varies depending on the underlying surface, usually land or water, where land-based convection tends to be shorter in duration.

A cumulus cloud has a complex structure consisting of several short-lived, individual plumes of rising air called thermals. These thermals are accelerated vertically and are non-hydrostatic, non-steady, and turbulent. As these plumes rise within the cloud, they carry, among other things, moisture and latent heat, which *entrain* into the cloud, modifying it through mixing. Positive

buoyancy, or instability, of the air in these thermals is dependent upon its density, which is affected by the environmental lapse rate. The lapse rate is defined as the rate of change of the temperature of atmosphere with height: dT/dz , where T is the atmospheric temperature and z is the geometric height. Also, the instability depends on the rate of mixing of air within the plume with the surrounding environment and on the water vapour and condensates in the cloud.

The stability of the atmosphere is important for cumulus convection. The atmosphere can be said to be in a metaphysical state, where potential energy is stored until released to give rise to violent convection – typically found in the midlatitudes. However, in the tropics, such violent convection is rare at best, which means that such a build of potential energy is smaller in magnitude. Therefore, forecasting tropical convection involves forecasting the evolution of such an energy source as well as a triggering agent. The energy source for convection is the availability of potential energy to a parcel until it reaches a level of neutral buoyancy. This is defined as the Convective Available Potential Energy (CAPE):

$$CAPE \equiv \int_z^{LNB} B dz = \int_z^{LNB} \frac{g}{T_v} (T_{vp} - T_v) dz = \int_{LNB}^p R_d (T_{vp} - T_v) d \ln p,$$

where B is the buoyancy force per unit mass, T_v is the virtual temperature, T_{vp} is the virtual temperature of a adiabatically displaced air parcel, p is pressure, R_d is the gas constant for dry air. LNB stands for the level of neutral buoyancy.

CAPE describes the kinetic energy an unstable parcel of air can attain as it rises through the atmosphere, if mixing is ignored and the parcel adjusts instantaneously to the local environmental pressure. However, CAPE is simply an indicator of the strength of convection. If the amount is low, the convection will be weak. What determines if convection is initiated or not depends largely on the vertical shear¹ of the horizontal wind near the surface.

The buoyancy of an air parcel depends on its density, which depends on the amount of water present in it. The virtual temperature is used to account for the presence of water and water condensates in an air parcel. If water vapor is increased/decreased at a constant temperature, the positive buoyancy and the virtual temperature increase/decrease. There is no simple way to measure the buoyancy of a rising air parcel. In processes involving a rising/subsiding air parcel, there are many atmospheric variables that are conserved. However, there is none that is a good measure of the buoyancy of

¹Change in wind speed with height.

a saturated, cloudy air parcel with respect to an unsaturated environment. Therefore, assessing the stability of moist convection must be done by other means, for example, the thermodynamic diagram, or computers, which is an estimate at best.

In the tropics CAPE is usually weak, so the release of latent heat fills the gap as the primary energy source for convection. This dependence on evaporation connects convection to the surface heating from the diabatic process of solar insolation. Convection releases latent heat into the atmosphere and creates a local response in the atmospheric circulation and excites equatorial waves. This creates a strong connection between tropical convection and the mesoscale and the large-scale circulation found in this region.

2.3 Equatorial waves

Some examples of equatorial waves that interact with convection via the exchange of latent heat are Equatorial Kelvin (EK), Equatorial Rossby (ER), and Mixed Rossby-Gravity (MRG) waves². EK waves are trapped at the equator and move eastward depending on whether or not convection is associated with them. These waves are fast moving if there is no convection, between $\sim 30 \text{ m s}^{-1}$ and 60 m s^{-1} , but significantly slower if there is accompanying convection, between $\sim 12 \text{ m s}^{-1}$ and 25 m s^{-1} . Convection is often found embedded in EK over, for example, the western Pacific and Indian oceans. The typical description of ER waves are alternating low and high pressure areas that are symmetric about the equator. Unlike EK waves, these waves move westwards between $\sim 10 \text{ m s}^{-1}$ and 20 m s^{-1} without accompanying convection and between $\sim 5 \text{ m s}^{-1}$ and 7 m s^{-1} otherwise. The dissipation of energy via MRG helps to sustain convection that are strong enough to reach the UT. These waves also move westward between $\sim 8 \text{ m s}^{-1}$ and 10 m s^{-1} .

2.4 Deep convection

The larger the cloud, the greater the effect it will have on the atmosphere. Convective clouds that penetrate the tropical boundary layer inversion, and whose level of neutral buoyancy lies at pressure levels $\lesssim 200 \text{ hPa}$ (10 km and 17 km), are called deep convective clouds [Folkens and Martin, 2005]. Deep convection can come from a single cloud or from organised cloud systems called clusters.

²See the MetEd Comet Program module on Equatorial Waves: https://www.meted.ucar.edu/tropical/synoptic/MJO_EqWaves/navmenu.php?tab=1&page=2.2.0&type=flash

These clouds, or cloud systems, often reach levels of the UT where the cloud top temperature is $\lesssim 235$ K. Since the anvil cloud from deep convection often covers an area large enough to be resolved by many satellites, deep convection is often identified by its cloud top temperature, [see e.g., Liu et al., 2007; Mapes and Houze, 1993; Soden and Fu, 1995, and references therein]. Further, since most of the precipitation in the tropics comes from deep convection [eg. Folkins and Martin, 2005; Hong et al., 2005], there is a strong correlation between the surface rain rate and such cloud systems. The factors that determine if a cumulus cloud grows into a deep convective cloud include the presence of low-level convergence (typically found in the ITCZ), enough CAPE, and the level of humidity in the column, especially in the lower troposphere (closely associated with the sea surface temperatures).

2.5 Tropical circulations

Large-scale circulation systems in the tropics have different characteristics from those found outside the region. There are several main large-scale circulations within the tropics. In addition to the ITCZ, which has already been discussed, these circulations are equatorial waves disturbances, African wave disturbances, tropical monsoons, Walker circulations, and the El Niño and the southern oscillation (ENSO).

Equatorial wave disturbances are transitory and move zonally within the ITCZ in the form of organised precipitation and sustained high level of cloudiness. Such waves are driven by the release of latent heat from condensating water inside deep convective clouds. This connection between deep convective clusters and equatorial waves is too complex to fully explore in this thesis. Cursively, equatorial waves contain the largest number of deep convective clusters and provide a *protected* environment for an air parcel to rise without much environmental entrainment, thus enabling deep convection to transport a large amount of latent heat and mass to near-tropopause levels.

While tropical waves disturbances behave similarly for most of the region, over Africa, the presence of the Sahara desert creates a strong baroclinic³ environment in the lower troposphere. This baroclinic zone, which is present during the strong diabatic heating of the summer months, gives rise to an easterly jet stream. Observations show that disturbances over the continent tend to move westward following this jet. Hurricanes that move through the Caribbean are often formed from these disturbances. One notable feature of African waves is that they draw energy from the conversion of energy between

³Baroclinic air masses are ones where the air density depends on both temperature and pressure.

the local baroclinic zone of the easterly jet and the general barotropic⁴ environment of the tropics.

Monsoons are periods of heavy precipitation that are driven by the land and ocean temperature contrast. A monsoon will occur where the hotter, rising air over land creates a low pressure area (heat low) of convergence that pulls in warm, moisture laden air from offshore. This onshore flow is seasonal and generates a large amount of precipitation where they occur. Monsoons are most pronounced over southeast Asia and the Indian sub-continent.

Walker circulation describes a circulation that is zonal in orientation (east-west). This circulation is driven by tropical deep convection and are caused by longitudinal variations in sea surface temperatures, which are themselves driven by changes in wind-driven ocean currents. Variations in the Walker circulation have been given the name "Southern Oscillation". During the Southern Oscillation changes in the wind-stress patterns over the oceans induce a circulation change that pushes cold water to warm areas and visa versa. This change in the ocean circulation and the subsequent sea surface temperatures has been given the name El Niño. These two phenomena are often referred to jointly as ENSO so as to address the total circulation system.

All of the above circulations interact with deep convective clusters at varying length and time scales, which allows for a modification of the environment of the local convective area. Such time and length scale modifications often involve moisture transport, momentum transfer, etc., and involve complex, two-way relationships between tropical waves and convection that are clouded in uncertainty (see [Thuburn \[2011, Fig. 1.1\]](#) for an illustration).

⁴Barotropic fluid is a fluid whose density is a function of only pressure. In the atmosphere this translate to a region where the air temperature is fairly uniform over a broad horizontal area.

CHAPTER 3

Satellite observations

In this thesis, several satellite observations, mainly polar-orbiting, are used in the evaluation in climate models. Satellite observations provide global coverage of the planet remotely and on a regular basis. This chapter gives a general overview of the satellite observations used in this thesis.

3.1 Satellite observations

Satellite measurements provide information of atmospheric and surface properties such as vertical profiles of temperature, trace gas concentrations, and cloud cover, in addition to surface precipitation, and radiation at the top of the atmosphere. These variables are measured using active lidar and radar sensors as well as optical, passive infrared, and passive microwave sensors.

Satellite sensors cannot measure the atmospheric quantities mentioned above directly. But the emission, absorption, and scattering of electromagnetic energy by constituents in the atmosphere allow for the derivation of geophysical parameters by interpreting the signal measured by the sensor. When the information required cannot be taken directly from the measurements, then the desired physical parameter needs to be retrieved. An inversion method is used to reconstruct the atmospheric state and derive the variable sought from the measured signal. A major complication is the fact that there can be many atmospheric states that give rise to the same measured signal. It is often the case that there are insufficient data to provide a unique solution to the atmospheric state. Some key elements of this inversion process are weighting functions and averaging kernels that vary in characteristics for each sensor type and measurement technique. Unfortunately, remote sensing observations suffer from errors, aliasing, and other limitations that introduce a degree of

uncertainty in satellite inversion results.

The measurement of atmospheric and surface variables is carried out by several different satellite sensors that also employ various techniques. The measurement of atmospheric temperature employs passive sensors that detect radiation emitted by, e.g., CO₂ at 15 μm . CO₂ is an ideal candidate because it is a uniformly distributed gas, and, therefore, its thermal emission is assumed to be a function of temperature for a given pressure. Another atmospheric gas that can be used to measure the vertical temperature profile is O₂.

Atmospheric water exists in all three phases, although the majority exists as a highly variable trace gas. In certain atmospheric conditions water vapor, liquid water, and ice can exist simultaneously, which complicates satellite measurements of water in its individual phases. Humidity profiles are measured using both microwave and infrared techniques. However, since the amount of water vapor that can exist in a parcel of air is bounded by the temperature via the Clausius-Clapeyron equation, in cold regions of the atmosphere water vapor concentration is low. This further complicates the measurement of humidity. Atmospheric humidity is sometimes retrieved as specific humidity, which is the absolute amount of water vapor, expressed in, for example, kg kg^{-1} , or volume mixing ratio, expressed as part per million (ppmv). Another way to define water vapor is by relating it to the relative humidity expressed as a ratio of the actual vapor pressure to the saturation vapor pressure, either with respect to ice or with respect to water. Relative humidity with respect to ice is used throughout this thesis.

Clouds are strong absorbers of thermal infrared radiation, and they are good at scattering radiation in the optical band. Atmospheric ice is found mostly inside clouds and contribute to the cloud's radiative properties. Both clouds and cloud ice can be measured passively and actively.

Passive emissions of microwave energy from the surface of the planet and the atmosphere are used to retrieve surface precipitation intensity. Infrared cloud-top temperatures (cloud heights) are correlated to surface precipitation to provide an additional measurements of surface precipitation. These various sources are combined to give full coverage of rainfall across the tropics.

3.2 Atmospheric infrared sounder

The Atmospheric Infrared Sounder (AIRS) provides height resolved humidity profiles [see e.g., [Gettelman et al., 2006, 2010](#)]. The horizontal resolution is approximately 45 km and the vertical resolution decreases with height from about 1 km near the surface to roughly 3 km near the tropopause. The sensor flies in a sun-synchronous polar orbit and crosses the equator (ascending and

descending nodes) at roughly 13:30 and 01:30 local solar time.

Specific humidity is retrieved from the sensor measurements and then converted to relative humidity using a Groff-Gratch formulation for saturation vapor pressure. A significant drawback to the AIRS humidity data is its sensitivity to cloud, which strongly absorbs infrared emissions. Consequently, humidity profiles are only available in situations where the cloud fraction is $\leq 70\%$. Further limitations have resulted in the retrieved humidity values being only scientifically useful at pressure levels $\gtrsim 200$ hPa [Gettelman et al., 2006]. These limitations on the data mean that AIRS does not provide full coverage of the upper troposphere nor is it usable when examining deep convective clouds systems.

3.3 Microwave limb sounder

The Microwave Limb Sounder offers the opportunity to measure upper-tropospheric humidity in the presence of clouds [Fetzer et al., 2008; Read et al., 2007]. The sensor measures microwave thermal emission from the upper troposphere and above at a frequency of 190 GHz. Its vertical resolution is roughly 4–6 km and has a horizontal resolution of 200–300 km and 6–12 km, along and cross track respectively. The sounder also sits in a sun-synchronous orbit with ascending and descending nodes similar to AIRS. Height resolved humidity profiles suitable for scientific study are obtained for pressure levels between 383 hPa and 0.002 hPa. Measured specific humidity is converted to relative humidity in a similar manner to AIRS.

3.4 AMSU-B and MHS

Similar to the MLS sensor, the Advanced Microwave Sounding Unit-B (AMSU-B) radiometer measures atmospheric microwave emissions. This is done for different altitudes using 5 channels (89.0 ± 0.9 , 150.0 ± 0.9 , 183.31 ± 1.00 , 183.31 ± 3.00 , and 183.31 ± 7.00 GHz). However, AMSU-B is downward-looking, whereas MLS is a limb (sideways-looking) sounder. AMSU-B are standard sensors onboard the National Oceanic and Atmospheric Administration (NOAA) and the European Space Agency polar-orbiting, sun-synchronous satellites. Microwave Humidity Sounder (MHS) is the next generation of AMSU-B sounder measuring atmospheric microwave emissions between 89 GHz and 190 GHz. In this thesis, AMSU-B and MHS are treated in a similar manner.

Humidity is retrieved from brightness temperatures measured by the sensor

[Buehler and John, 2005; Buehler et al., 2008]. A linear equation is used to map the sensor measurements to relative humidity, but for these retrievals, the interpretation is not straightforward. The weighting functions are dependent on the atmospheric state; thus, in drier conditions, the measurement is representative of altitudes lower down in the atmosphere. Therefore, this mapping of the sensor signal to humidity is not defined for only one specific altitude. Consequently, AMSU-B/MHS humidity is defined as a weighted mean for the upper troposphere.

3.5 Cloud profiling radar

A cloud profiling radar measures backscatter reflectivity as a function of distance to a cloud or ice particle. The CloudSat satellite employs such a radar to measure atmospheric hydrometeors at 94 GHz (3 mm) with a vertical resolution of about 240 m and a horizontal resolution of ~ 2 km [Stephens et al., 2002]. The CloudSat retrieval algorithm is described in Austin et al. [2009]. The satellite is placed in a sun-synchronous polar orbit with equatorial crossing (ascending/descending) times of approximately 13:30/01:30 local. The sensor's sensitivity to precipitation is size dependent such that, the larger the ice particles, the greater the backscattered signal. This sensitivity limits CloudSat's usefulness in the upper troposphere where ice particle sizes are small.

While CloudSat can penetrate any cloud to reveal its 2-D structure, there is unfortunately a 40% retrieval uncertainty, which is a result of marginal information on the ice particle size distribution. Additional uncertainty is caused by the sensor's inability to detect the phase of the hydrometeor generating the backscattered signal. The partition between liquid water and ice, a part of the retrieval process, is a linear function of temperature. Above 273 K, the profile is assumed to contain only liquid water whereas below 253 K, solid ice is assumed.

3.6 Cloud profiling lidar

Cloud-Aerosol Lidar with Orthogonal Polarization (CALIOP) is a polarization-sensitive lidar that measures vertical profiles of aerosols and clouds [see e.g., Chepfer et al., 2010; Winker et al., 2007]. Profiles are measured using two channels to measure polarized backscatter signal at 532 nm wavelength and another at 1064 nm. The sensor is onboard the CALIPSO satellite and detects clouds with an optical depth < 0.01 . Because of its high sensitivity to optically

thin clouds, the CALIOP sensor saturates quickly in cloud conditions. Cloud profile of the upper troposphere is obtained by combining cloud information from CloudSat and CALIOP.

3.7 TMPA

More than 60 % of the planet's rainfall occurs in the tropics, which is also the region with the most incoming shortwave radiation. Water releases a large amount of energy when it changes phase, and the tropics attain radiative-convective balance by the release of latent heat transported aloft during convective events. This cycle of evaporation and condensation is an integral part of the hydrological cycle and mapping the cycle of rainfall in the tropics is very important. The Tropical Rainfall Measuring Mission (TRMM) employs visible, infrared, and microwave sensors to measure rainfall in the region. Surface rain gauge measurements are then used to validate the remotely sensed rain estimation techniques.

Three rain measuring instruments fly onboard the TRMM satellite:

1. Visible and Infrared Scanner provides high resolution observations on cloud coverage, cloud type, and cloud top temperatures.
2. TRMM Microwave Imager provides integrated column precipitation, cloud liquid water, cloud ice, rain intensity, and type of precipitation.
3. Precipitation Radar measures the 3-D precipitation.

The satellite is placed in a relatively low orbit that is not sun-synchronous. The low inclination of the satellite orbit provides coverage between $\pm 35^\circ$ latitude, a choice to give greater coverage of the tropics. However, complete spatio-temporal coverage of the tropics is not attainable with just one satellite. The Tropical Rainfall Measuring Mission (TRMM) Multisatellite Precipitation Analysis (TMPA) [Huffman et al., 2007] combines precipitation data from many more sensors to obtain a tropical precipitation analysis with a high spatio-temporal resolution ($0.25^\circ \times 0.25^\circ$ at 3-hour intervals). Other polar-orbiting sensors that contribute to the TMPA dataset are NOAA's AMSU-B, Special Sensor Microwave Imager (SSM/I) on Defense Meteorological Satellite Program satellites, and Advanced Microwave Scanning Radiometer-Earth Observing System (AMSR-E) on the Aqua satellite. Together, these satellites are still not able to obtain full spatio-temporal coverage of the tropics. Precipitation data derived from infrared sensors onboard geo-synchronous earth orbit satellites fill in the gaps and allow the TMPA dataset to provide full spatio-temporal coverage.

3.8 CERES

Radiation at the top of the atmosphere is measured by the Clouds and the Earth's Radiant Energy System (CERES) [Loeb and Kato, 2002]. This instrument is based in a previous instrument called Earth Radiation Budget Experiment (ERBE). CERES is a scanner housing three detectors that measure shortwave radiation ($0.3 - 5.0 \mu\text{m}$), longwave radiation $8 - 12 \mu\text{m}$, and total radiation ($0.3 - 100 \mu\text{m}$) channel. The sensor flies onboard two satellites, Terra and Aqua, and crosses the equator at 10:30/22:30 local solar time for Terra and 13:30/01:30 local solar time for Aqua. The sensor scans from limb to limb cross-track and scans along track using a 360° azimuth biaxial scan.

3.9 Sampling error

Convection in the tropics an integral part of this thesis. An important aspect of convection in this region is its diurnal cycle, which requires consistent spatio-temporal coverage in order to be resolved properly. However, this is often not the case for polar-orbiting satellites, especially those in sun-synchronous orbits [Kirk-Davidoff et al., 2005], e.g., CloudSat. This low-frequency diurnal sampling causes random errors and biases in retrieved atmospheric variables associated with convection. Increasing the diurnal sampling greatly reduces this problem, however, consideration must also be given to the sensor's scanning pattern. Because the composites used in this thesis cover a broad geographical area, sensors with narrow swaths will not adequately cover the composite's spatial domain, which further contributes to aliasing effects.

CHAPTER 4

Atmospheric General Circulation Models

This section gives a very brief description of the numerical model used to approximate the atmospheric component of a climate model. The section is limited to just a few aspects of this model component as they pertain to the subject of this thesis.

4.1 Background

The average weather pattern of a region defines its *climate* and does this in terms of the longterm mean and variability of, for example, temperature, precipitation, and wind. The *climate system* is an interactive system consisting of the atmosphere, lithosphere, hydrosphere, and biosphere. Energy from the sun drives the climate system and changes in this system are caused by internal (e.g., changes in greenhouse gas concentrations) and external (e.g., volcanic eruptions or solar variations) forces. As these forces are applied to the climate system, its responses can both be direct or indirect via feedback mechanisms. The response in these systems all occur at different temporal and spatial scales. Figure 4.1 show the typical response time to changes in the climate system.

Future climate projections require knowledge of key climate system component processes and the interactions between them. In the atmosphere, governing equations that describe the conservation of mass, momentum, and energy are expressed in a numerical environment called a *model*. Atmospheric general circulation models are therefore numerical systems that describe the processes necessary to simulate the climate system component.

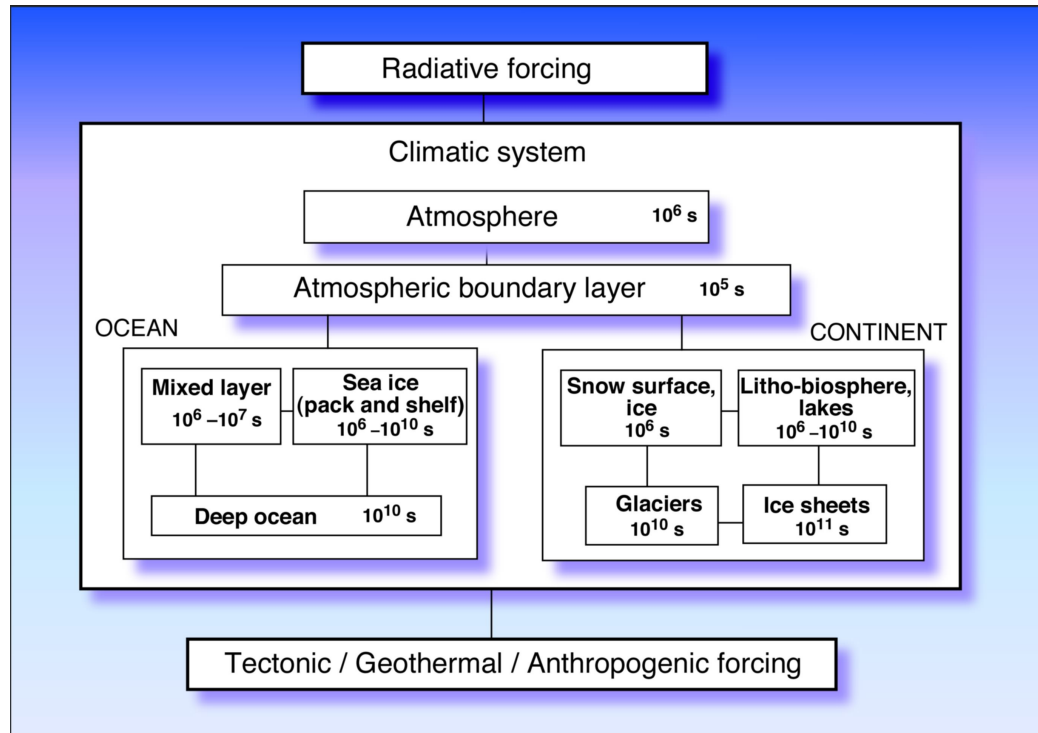


Figure 4.1: A schematic representation of the domains of the climate system showing estimated response times. Source: *McGuffie and Henderson-Sellers [2005]*.

There are several types of models that can be used to study the atmospheric climate component. Some examples are, in order of increasing complexity, energy balance models (EBM), radiative-convective models (RCM), statistical-dynamical models (SDM), and atmospheric general circulation models (AGCM) [Meehl, 1984]. EBMs and RCMs are often used to study the global energy exchange, the planet's effective emissivity, and atmospheric profile. SDMs are usually a combination of a EBM and a RCM but with increased dimensions. AGCM may be run using prescribed boundary conditions instead of being coupled with other models such as an ocean or ice model. But any study of the real climate can only be done using a AGCM coupled to models that describe the other climate system components (see Fig. 4.1).

Since the mid 1950s, climate models have become increasingly complex by trying to incorporate more and more systems and processes thereby significantly increasing the number of equations, and parameterizations. Figure 4.2 illustrates the evolution of climate models since the early 1970's. The ever increasing complexity of AGCMs is needed to simulate a climate system with multiple interactions and feedbacks. At the same time, the increased

complexity makes interpreting model output more difficult.

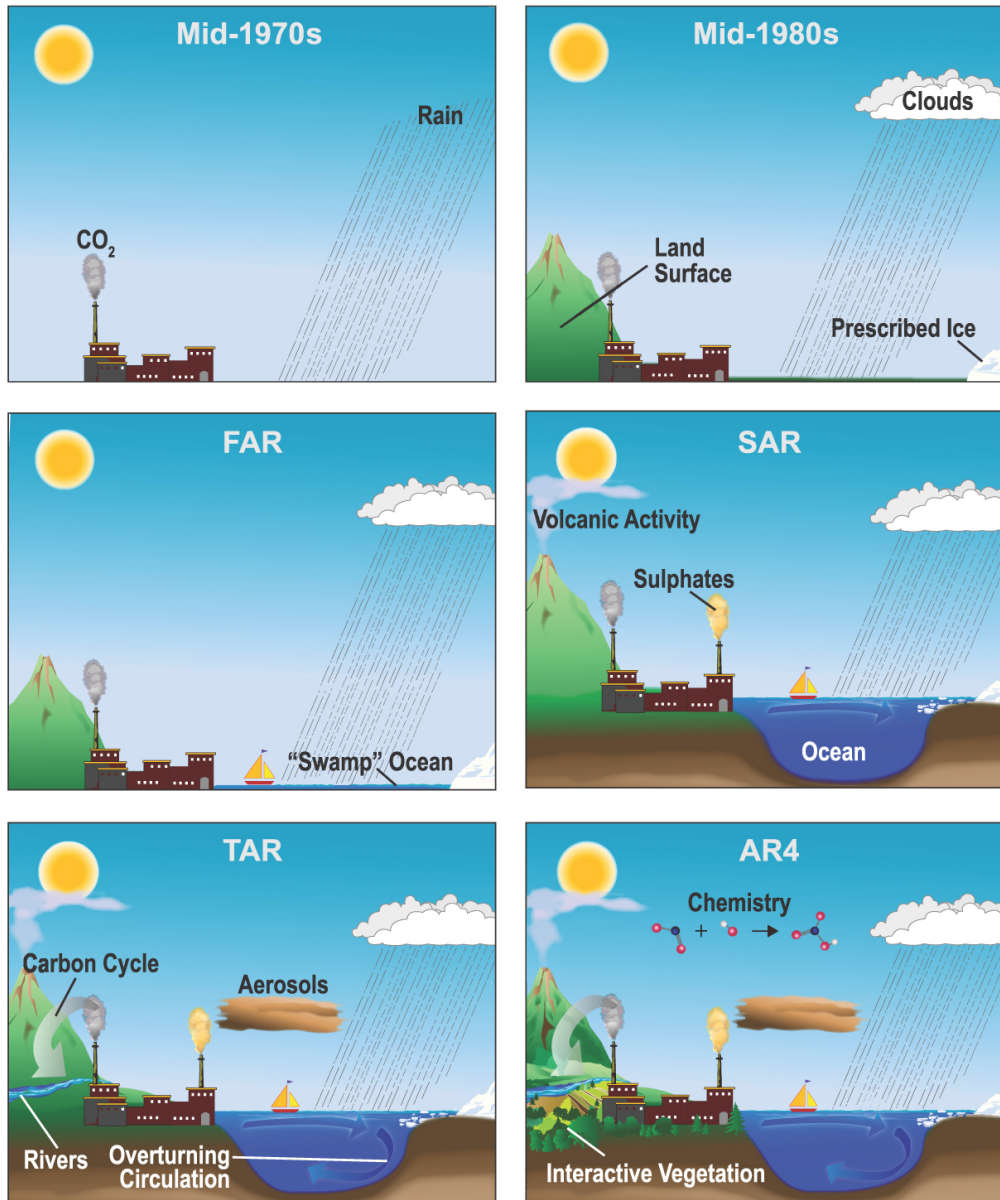


Figure 4.2: Evolution of general circulation models since the 1970's. The added parameterizations (physics) are shown pictorially by the different features of the modelled world. Source: IPCC WG I

4.2 Dynamics and physics

AGCMs must contend with the dynamics of a fluid on a rotating planet, the physics behind each process, the energy balance between the planet's outgoing longwave and the incoming shortwave radiation, plus the redistribution of energy throughout the atmosphere. At any point in time, AGCMs represent winds, atmospheric density, pressure, temperature, and humidity. This is the dynamics of the model and is concerned with mass continuity, water conservation, momentum, and internal energy. In the governing equations, there are four independent variables: time (t), height above sea-level, or geopotential (Φ), longitude (λ), latitude (ϕ). There are seven dependent variables, namely horizontal velocities east-west v and north-south u , vertical velocity ω , density, ρ , mass water (ice, liquid, and vapour) q , temperature, θ , and pressure, p .

With seven dependent variables there are therefore seven basic equations climate models must solve for the atmosphere on a rotating Earth. Atmospheric motions caused by differential heating from the sun are solved using the *momentum* equation. If we let \vec{U} represent the vector components of velocities (v, u, ω) and Ω is the rotation speed of the planet, then the three dependent variables can be solved using the expression

$$\frac{d\vec{U}}{dt} = \underbrace{-2\Omega \times \vec{U}}_{\text{Coriolis}} - \underbrace{\frac{1}{\rho} \nabla p + \vec{g}}_{\text{PGF}} + \vec{F}_r, \quad (4.1)$$

where the first term is the Coriolis effect, the second is the pressure gradient force (PGF), third term is the net force of gravity that includes centrifugal force, and last term is frictional drag. This is an atmospheric expression of Newton's second law of motion ($\vec{F} = m\vec{a}$) and includes an advection term ($\frac{d}{dt} = \frac{\partial}{\partial t} + \vec{U} \cdot \nabla$).

Another equation for the fourth dependent variable ρ describes the conservation of mass and states that the local rate of change of density is equal to minus the mass divergence is given by

$$\frac{\partial \rho}{\partial t} + \nabla \cdot (\rho \vec{U}) = 0, \quad (4.2)$$

where ρ is the local atmospheric density. A third equation describes the conservation of constituents such as water mass and represents one of the most difficult aspects of modelling. The implementation of these equations vary from model to model and an example can be written for specific humidity q as

$$\frac{\partial \rho q}{\partial t} = \underbrace{-\nabla \cdot (\rho q \vec{U})}_{\text{Advection}} + \underbrace{E - \rho C}_{\text{Source \& Sink}}, \quad (4.3)$$

where E is a evaporation/sublimation, and C is condensation/deposition. This flux form for water mass conservation (using Eq. 4.2), represents a balance of temporal and spatial changes with sources and sinks. In models such EC-Earth, where the treatment of precipitation is diagnostic, humidity and cloud water (e.g., ice and liquid combined), or cloud ice and cloud liquid water, would be represented by two such equations.

A fourth equation describes the thermodynamics that governs the conservation of energy with respect to a moving air parcel defined as

$$Q = C_p \frac{d\theta}{dt} - \frac{1}{\rho} \frac{dp}{dt}, \quad (4.4)$$

where C_p is the specific heat capacity, and Q is the heating rate per unit mass. The equation of state $p = \rho RT$ is the final equation and describes the relationship between temperature, pressure, and density for an ideal gas.

These governing equations are solved for each time step as well as spatially but are limited by computational cost and processing time in order to make modelling the atmosphere practical. The next step to solving the governing equations involves some necessary approximations that are standard in climate models. Some approximations are the *hydrostatic relation*:

$$\rho g = -\frac{dp}{dz}, \quad (4.5)$$

where, g is acceleration due to gravity and ρ is the density, that states that at large spatial scales, typically > 10 km, vertical acceleration is negligible; the vertical component of the *Coriolis effect* can be ignored; and the *quasi-Boussinesq* approximation that states: variations in atmospheric density in time are very small compared to other components of Eq. 4.2, which in effect filters out sound waves.

The governing equations so far do not address some important aspects of the atmosphere such as clouds and radiation. Therefore, more equations that describe missing elements are added. At this point, the model system is not closed since the energy dissipating frictional force, \vec{F}_r , and heating rates from the sun and the Earth's surface, mixing, as well as transport of heat that arises from phase change in water are still unspecified. To account for heating from the sun, the cooling of the planet, phase change heating and cooling from primarily convection a *radiative-convective transfer model* is

added. The addition of clouds, convection and radiation are often referred to as the model *physics*.

As mentioned earlier, AGCMs solve the governing equations on spatial and temporal scales that are partially determined by computational costs and numerical limitations. These scales are, today, on the order of tens to hundreds of kilometres with time steps from several minutes to about an hour. Without the above limitations, the equations being solved can provide information down to \sim cm scale and on time steps on the order of seconds. This disparity between what the model scale resolves from the equations, plus the fact that many important variables, such as clouds, occur at multiple scales, including scales well below 50 km (resolution of next generation AGCMs), require the addition of more equations. Any additional equations to the original seven is one form of *parameterization* (Sect. 4.3). These types of parameterizations require closure that is achieved when boundary conditions that describe the interactions of other components of the climate system are added. Figure 4.3 illustrates the different components of several major climate systems and the processes that must be represented.

4.3 Parameterization

In order to adequately represent the atmosphere in a numerical model, the basic governing equations need to be supplemented with equations that describe other processes that are not covered but are equally important. These additional equations are called *parameterizations*.

Parameterizations can be described as simplified models of unresolved processes that can be measured or not. An example of parameterization is convection that account for the vertical transport of momentum, heat, and total water. A second type of parameterization is radiation, which involves processes that affect molecular internal energy, a kind of diabatic process, i.e., absorption/emission of photons and phase changes. The third kind of parameterization in AGCMs are additions to the governing equations. Examples of these are land surface scheme, carbon cycle, clouds effect, chemistry, and aerosols. Parameterizations in AGCMs reflect, from their design, use, and implementation, our understanding of the processes they describe. Many of these processes are not well understood and therefore parameterizations become a source of uncertainty in AGCMs. Thuburn [2011, Fig. 1.1] illustrates the gap that parameterizations must bridge in the models. The darker-shaded areas, that represent spatio-temporal scales of various models, are noncontiguous, but the lighter-shaded area, that represents nature, is contiguous. Parameterizations bridge the gaps between these darker areas. AGCMs today

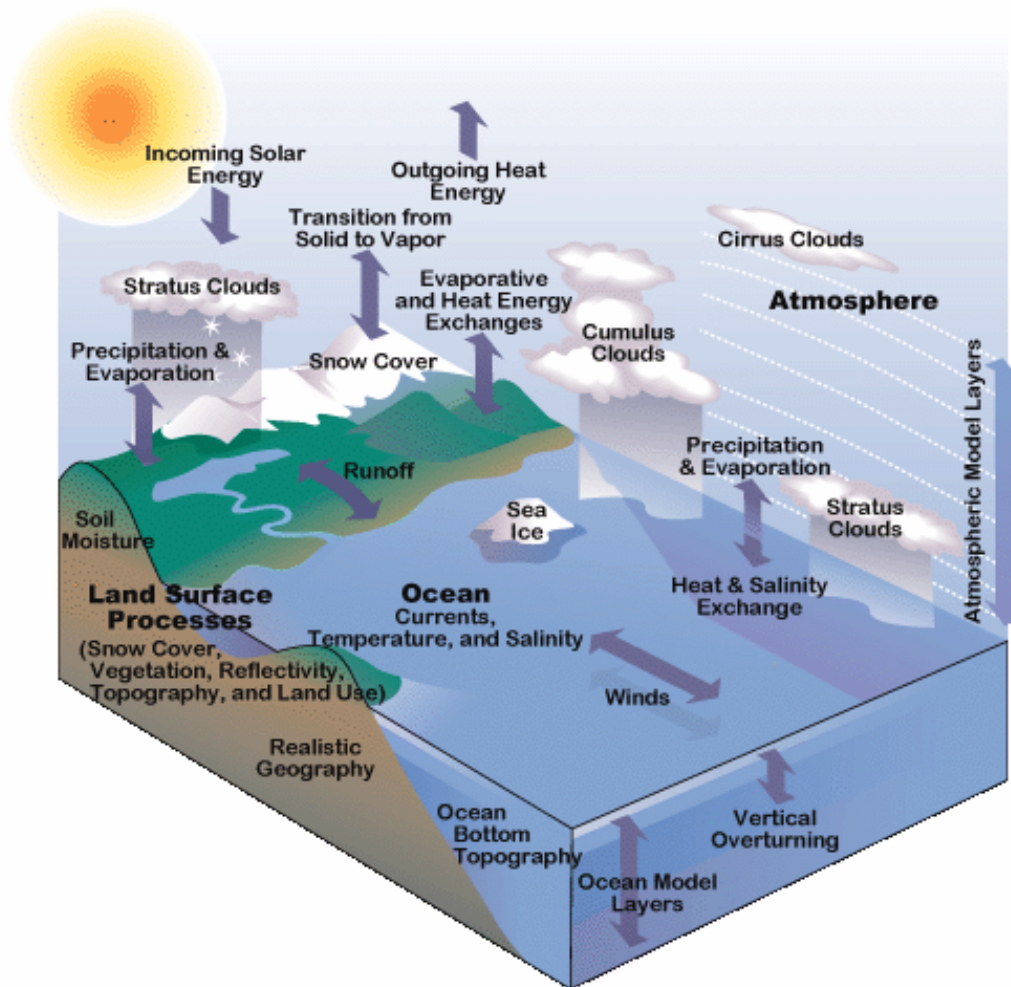


Figure 4.3: *Typical numerical model domain for a coupled system. Source: NCAR CCSM*

have a typical resolution of ~ 100 km and a time step of about ~ 1 h. This puts current AGCM resolutions at the same level as cloud clusters.

4.4 Clouds

The role of clouds in the atmosphere is complex and broad. Clouds affect the 3-D dynamics, temperature, humidity, radiation, and the water budget in the atmosphere. The effects of clouds on the global climate depend on their amount, location, height, lifespan, and optical properties. The radiative impact of clouds is not only dependent on the above cloud properties, but

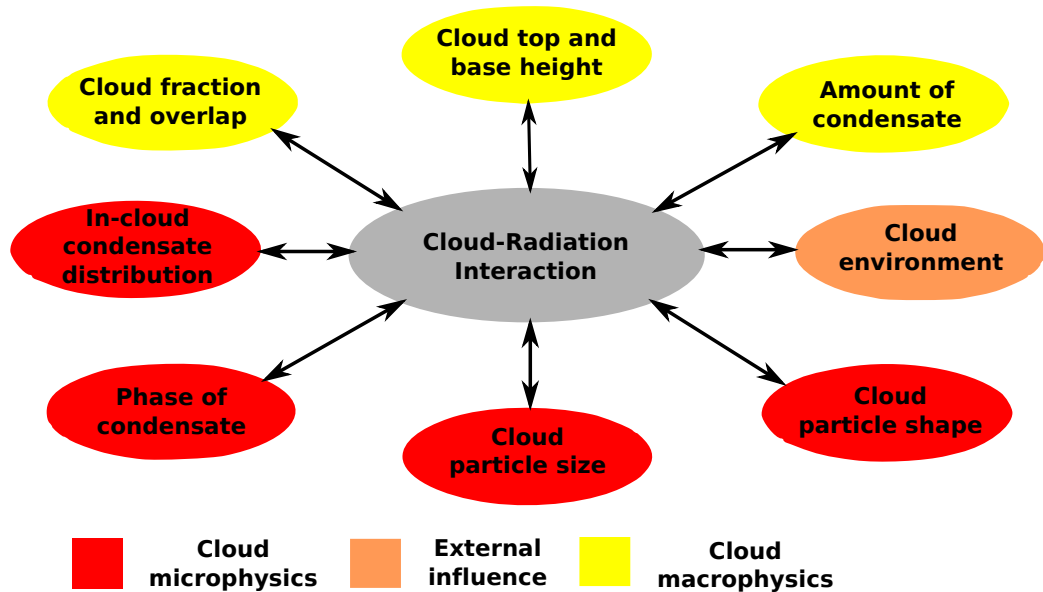


Figure 4.4: *Cloud-radiation interaction, the processes involved, and the scale at which they occur. Red: microscale, yellow: macroscale, grey: quantum scale.*

also the time of year and day. The optical properties and radiative impact are also dependent on the presence of aerosols.

Simulating clouds and cloud effects are very difficult tasks that many AGCMs solve in a similar manner but with small yet significant differences. It is common to link the cloud formation to the relative humidity as it rises above a particular threshold, and the interaction with aerosols is often simplified, if represented at all. Explicit cloud representation has only been implemented in AGCMs since the early 1980s based on work by Sundqvist [1978]. The effect of clouds in models is usually encompassed in three processes: cloud fraction, cloud microphysics, and cloud radiative properties [Kiehl et al., 1998]. Figure 4.4 shows an example of the processes involved in cloud-radiation interaction and the scales on which they occur. However, micro-properties of clouds exist at scales that are smaller than the resolutions of contemporary AGCMs. Therefore, many AGCMs employ parameterizations (see Sect. 4.3) to describe these sub-grid properties. Parameterizations of clouds describe statistical properties of a cloud field, but neglect individual cloud elements. The goal, however, is to simulate the clouds as realistically as possible. Because many of the processes involving clouds are still poorly understood, cloud parameterization is the largest source of uncertainty in AGCMs [Bony et al., 2006].

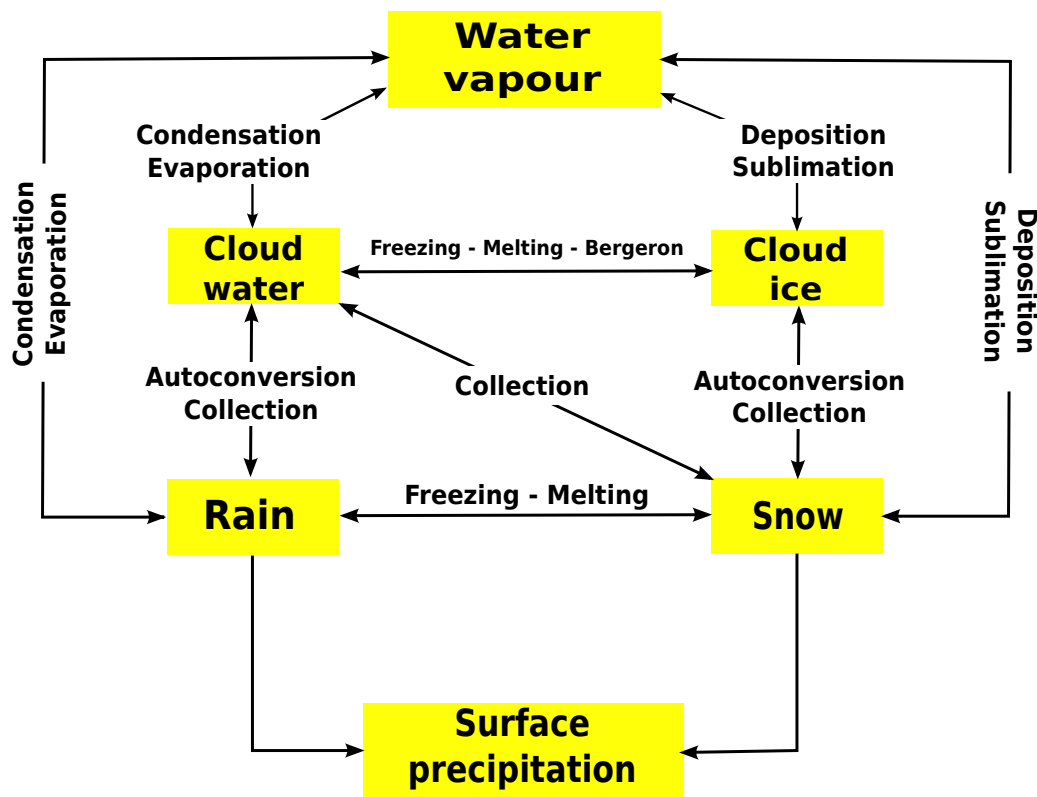


Figure 4.5: Schematic of a microphysical parameterization with water vapour and four categories of condensation/hydrometers. Source: [Forbes, 2009].

4.4.1 Cloud microphysics

The microphysics of a model refers to its ability to simulate cloud and precipitation processes. The effects of clouds extend to the molecular levels and fall under the category of cloud microphysics. This area of clouds formation covers processes such nucleation (homogeneous and heterogeneous), supersaturation with respect to ice and water, and the effects of different aerosols present in the atmosphere. The difficulty of cloud microphysics increases in the ice phase with the addition of more complex ice shapes and sizes. Since the distribution of water/ice is important in a grid box, further complications arise in the regions where both ice and liquid coexist simultaneously (mixed phase generally between 250 and 273 K). Microphysical parameterizations aim to represent these combined molecular effects in a grid box. Figure 4.5 illustrates a schematic of a microphysical parameterization.

4.4.2 Model uncertainty

Poor understanding of many of the microphysical processes illustrated in Fig. 4.5 contribute to much of the uncertainty surrounding climate model simulations.

Also, GCMs must balance the computational efficiency of each parameterization with accuracy. Complex parameterizations can be costly and there is no guarantee that a more detailed approximation, which takes into account many micro-processes, would result in a better representation than a simpler, less detailed one. That is to say, improvements in any parameterization is limited to the level of detail available inside the model. Uncertainty can be found in every aspect of numerical models which means that AGCMs can be sensitive to changes in the formulation of their parameterizations.

4.5 Cumulus parameterization

AGCMs account for the vertical redistribution of temperature and moisture and the reduction of atmospheric instability via cumulus parameterization. Special attention is given to this parameterization because it is one of the largest source of uncertainty in climate projections [e.g., [Bechtold et al., 2008](#); [Randall et al., 2003](#); [Tost et al., 2006](#)]. It is a daunting task for AGCMs to produce a fair representation of cumulus convection. An overview of cumulus convection in this region of the planet is given in Chapt. 2. Figure 4.6 illustrates some general properties of convection that cumulus parameterizations must represent. Convection at the typical grid scale of ~ 100 km is implicit and the objective AGCMs is the representation of *apparent source*, which is to say that models treat sub-grid convection statistically and balance it with prognostic variables¹ at grid scale.

There are many types of convective schemes, but all must account for transport of heat and increase the stability of the column. Using grid-box mean data, the scheme determines a trigger for convection, determines how ongoing convection adjusts column temperature and humidity profile, and determines how convection and grid-scale dynamics interact with each other.

It is common practice to simulate convection using a bulk mass flux method. The cumulus clouds are represented by an ensemble of cloud updraft and downdraft plumes. In some models, even a single pair of plumes are employed instead of an ensemble. These plumes describe the entraining² and

¹Variables whose update at each time, t , includes its value from time step, t_{-1} , i.e., variables with history.

²The mixing of environmental air into the cloud.

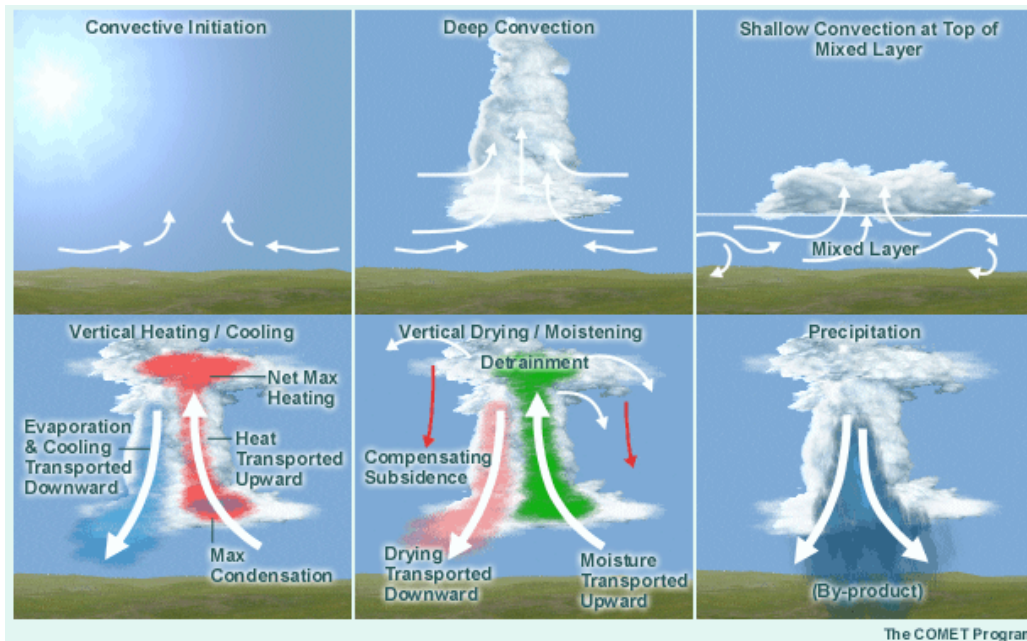


Figure 4.6: Schematic depiction of some processes associated with convection that must be account for in cumulus parameterization (CP) schemes. Source: Comet Program (http://www.goes-r.gov/users/comet/tropical/textbook_2nd_edition/navmenu.php_tab_10_page_4.6.0.htm).

detraining³ of moisture, heat, and condensates. Convection in AGCMs is generally either shallow or deep, depending on several factors such as the height of the level of neutral buoyancy (level of detrainment). Some models even simulate mid-level convection, which is a type of convection whose base is found above the planetary boundary layer⁴.

Convection inside the grid box of a AGCM impacts a model's large-scale circulation. At the same time convection itself is impacted by the large-scale circulation. Cumulus parameterization connects the convection to the large-scale circulation and does this by using closure assumptions. The main difference between the various cumulus parameterizations schemes that exist is the different types and formulations of closure assumptions they employ. One example is the assumption the convection reduces the amount of CAPE in the grid box.

³The opposite to entrainment.

⁴The lowest part of the atmosphere whose behavior is directly influenced by the surface.

CHAPTER 5

Summary and outlook

The overall goal of this thesis is the support of model development and assessment of satellite observations used in the pursuit of this goal. The focus is placed on simulated tropical upper-tropospheric (500 hPa to the tropopause) water and the outgoing longwave radiation. In this region of the atmosphere, the water goes through diurnal and seasonal cycles as it is affected by convective events and is known to be problematic. In the tropics the primary weather phenomenon is moist convection that is concentrated in a zone of large-scale, low-level wind confluence called the InterTropical Convergence Zone (ITCZ). There are several types of convection found in the tropics of which only deep convection has the energy, length, and time scales large enough to influence small- and large-scale processes in the upper troposphere (UT). This region of the atmosphere is difficult to observe, and global observations are exclusively provided by satellites. Satellites can provide many different types of atmospheric information, but they also have limitations such as cloud penetrability, spatio-temporal coverage, as well as measurement uncertainty. Nevertheless, satellite observations are a valuable component in climate model evaluation. Representation of upper-tropospheric water has been identified as problematic for climate models, and since this region of the atmosphere is mainly moistened by deep convection, the model's convection and cloud schemes are brought into focus. The thesis is built on three papers dealing with the evaluation of climate models with the aid of satellite observations in this atmospheric region. A summary of each of these papers is given in following section, and this chapter concludes with an outlook for future studies in connection with this work.

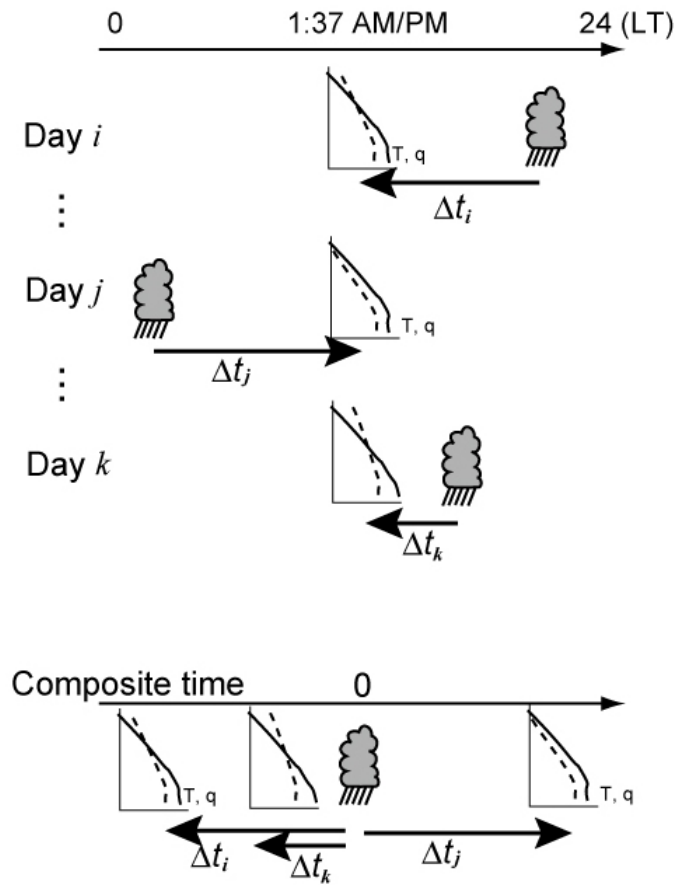


Figure 5.1: Construction of a composite from data collected for three days, i , j , and k at various times relative to peak convection, t_0 , indicated by a cumulonimbus cloud. Source: taken from the Gordon Research Conference: Radiation and Climate, July 8, 2013, based on Masunaga [2013].

5.1 Longterm mean and composite

It is very common to evaluate climate models using longterm means. Such methods involve averaging the model data over a time span before comparing it to observations. Longterm means reduce the signal of time periods that are not representative of the climatic mean, for example, El Niño years. While this method is useful in revealing disparities, much information is lost in the averaging.

Compositing, on the other hand, provides the opportunity to examine the evolution of deep convection in both space and time simultaneously. The method is simply the juxtaposition of snapshots of small of geo-spatial images to create a bigger picture, either in space or time. To begin with, a convective

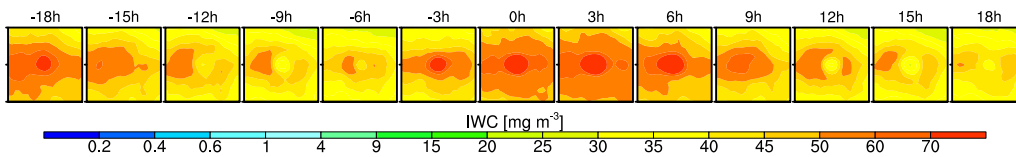


Figure 5.2: *Composite example of EC-Earth’s stratiform cloud ice at 200 hPa over central Africa. The composite displays a spatio-temporal coverage of ± 18 hours at every 3-hour interval and $\pm 10^\circ$ longitude and latitude taken from the centre point and graduated every $\pm 1^\circ$.*

event centered at a fixed location (a Eulerian frame) is sampled in a $\pm 10^\circ$ latitude and longitude window. In order to create a composite, the location is sampled at different times over a period of 96 hours at 3-hour intervals. The result is a spatio-temporal composite that covers the mean evolution of the convective events from initiation to dissipation. Figure 5.1 illustrates how such a composite is built. This method retains some information about variability of the systems and is a step closer to the convective processes being examined [see e.g., Field and Wood, 2007]. A composite method has been employed in much of the work that makes up this thesis. Figure 5.2 shows an example of a composite of simulated stratiform cloud ice over central Africa. For polar satellite observations, this method poses a problem because polar satellites take snapshots of the planet that are not contiguous in space and time. A composite of a single observed convective event is therefore of little use. Full spatio-temporal coverage is obtained by taking the mean over thousands of convective events.

5.2 Variable definition problem

The observations and simulated variables are often defined differently, which creates a problem when comparing the two. For example, clouds detected by microwave radar, infrared or microwave emissions, and lidar will all differ due to difference in the physics involved. The Moderate Resolution Imaging Spectroradiometer (MODIS) aboard NASA’s Terra satellite defines optically thin clouds as those with an optical depth of < 0.3 [Sun et al., 2011], whereas CALIPSO can detect clouds with much lower optical depth. Models also define optically thin clouds with varying thresholds. Therefore, comparisons between model and observations will be flawed if both definitions do not fully overlap.

Another atmospheric variable that suffers from similar definition problems is cloud ice water content. CloudSat measures cloud ice water content as a

function of the strength of the backscatter of its radar signal and is sensitive to a ice particle diameter size of $\sim D^6$. This translates to a sensitivity to large ice particles, which is commonly found in convective events. Most, if not all models, treat such large ice particles diagnostically, thereby excluding them from their standard cloud ice water content output. However, definition problems are mitigated if the differences between the simulated and the observed variable are small or considered insignificant, i.e., if one is only interested in certain properties of the variable such as spatial coverage, as it can be in the case of ice water content.

5.3 Appended papers

5.3.1 Paper I

The use of multiple observation sources allows for several tropical upper-tropospheric, water-based variables to be examined in parallel as well as providing a more complete coverage of the UT. Studies of this kind are not often done and, further, offer the opportunity to examine changes in upper-tropospheric variables, both observed and simulated, in relation to each other. The goal of Paper I is towards a robust assessment of upper-tropospheric observations and contributing to climate model development by evaluating simulated water cycles in this problematic area and is published as part of an EC-Earth special issue. Data from primarily the A-Train suite of satellites, the reanalysis dataset Era-Interim from the European Centre for Medium-Range Forecasts are employed, and a newly created cloud fraction dataset derived the CALIPSO lidar and called the GCM-oriented CALIPSO cloud product (GOCCP), are employed.

The seasonal vertical profiles and the horizontal distributions of upper-tropospheric water at primarily 200 hPa and 400 hPa are examined. In addition, the effect changes in the upper-tropospheric water has on the outgoing longwave radiation (OLR) is also examined. This is performed for several special regions in the tropics. These areas are distinguishable by their surface types, which are ocean and land. The article discusses the strengths and weakness of the observed data along side those of the climate model EC-Earth (version 2). Longterm means are used in a *retrieval to model* comparison for the four annual seasons over a 2-year period.

The simulated humidity profile showed good agreement with the observations. However, observed profiles contain large uncertainties as both datasets do not cover the entire UT and both sample the region using two very different techniques. The study also found large regional difference in the observed

effect of clouds on the OLR, but these areas of disparity are not always collocated with the modelled results. Nevertheless, the model captures the large-scale features and convective contributions to the diurnal and seasonal cycles of upper-tropospheric water.

5.3.2 Paper II

Paper II continues the use of multiple observations of upper-tropospheric water, but focuses more on observations of in-cloud properties and only for deep convection over the central Pacific. The paper assesses the evolution of tropical deep convection and its impact on upper-tropospheric moist processes in a statistical manner. While this work is not the first to examine the evolution of observed or simulated deep convection, we adopt and improve upon a composite technique used to identify deep convective (DC) system. In addition, the study also focuses on observations with in-cloud properties and is one of the first to use a particular UTH dataset from the Advanced microwave sounding unit/Microwave Humidity Sounder (AMSU/MHS) sensors. This work builds on Paper I by focusing on DC systems and advances the study a step further by being the first to examine simulated convection in such a manner and applying the methodology to the climate model EC-Earth (version 3).

Paper II employs the composite technique described in Sect. 5.1 that allows for high spatio-temporal resolution of the mean deep convective systems to be achieved. However, gaps in the observational coverage means that full spatio-temporal coverage of observed deep convection is only obtained statistically. When applied to the model, the results demonstrated that this important feature of the tropics can be isolated and evaluated from multiple perspectives.

The observations illustrate the effects of deep convective systems that can increase the background humidity and cloud fraction by about 20 and 7 percentage points respectively. Corresponding increases in cloud ice, albedo, and decreases in OLR also highlight the importance of deep convection for upper-tropospheric water. However, the study revealed a problematic aliasing effect, especially with single sun-synchronous satellite observations.

The composite method is successfully applied to the model that is able to capture the essential signatures of the DC systems' anomaly, in good agreement with the observations. Nevertheless, the model UT is often more moist, and near the tropopause the cloud fraction is greater than observed. Furthermore, simulated DC systems tend to move in the opposite direction than that observed. The modelled upper-tropospheric variables do not demonstrate similar cross-correlation as the observations, but despite this fact, the simulated OLR remains in good agreement with the observations.

5.3.3 Paper III

Paper III is a continuation of Paper II and is primarily focused on diagnosing the effect of deep convection on upper-tropospheric moist processes in the simulated atmospheres of EC-Earth (version 3), ECHAM6, and CAM5. The methodology of Paper III is the same as Paper II and carried out over the same time period.

While the previous study was only concerned with ocean-based deep convection, this paper takes a step further and examines land-based deep convection as well. Since climate models handle the simulation of deep convection in various ways, the study increases its significance by including three prominent climate models with different solutions to the convection problem.

The simulated effects of DC systems on the OLR agree reasonably well with the observations despite being generally higher than observed. The known issues of higher CF and lower IWC at 200 hPa, relative to the observations, remain, and the different environments over land and ocean that are conducive to DC systems are not handled well by the models. Over ocean the models perform better, but over land the major problem is the repetition of DC systems at the same geographical location roughly every 24 hours. The cause/causes of these problems remain elusive as there is no one-to-one relationship between the simulated UT variables and the surface rain rates.

5.4 Outlook

Through out this thesis, observations and model output for upper-tropospheric water, surface rain rates and OLR have been compared. Each time the goal was to contribute to model development by identifying areas where the model representation fails, or is weak, and, if possible, suggest ways to improve it. In parallel, the observations have been assessed and new datasets have been used or employed in a novel way. However, both the model output and observations complicate the evaluation in ways that make a robust comparison difficult. This section discusses a few ways to improve upon any future study that hopefully will arise from this thesis.

Simulated and satellite observation variable definitions do not often match. The problem of definition is greater for cloud ice water content, than for other upper-tropospheric variables. Simulated cloud ice exists in different forms, based on the meteorological conditions under which it is formed, and not all ice are prognostic in the models. This means that each model's standard output for ice water content will contain different parts of the ice particle spectrum.

Theoretically, such a problem could be partly addressed by removing the observations component that is missing in the model's definition. This can only partially solve the problem, since the delineation between the different ice components in the model is often ill-defined. The use of a pseudo-satellite radiance simulator in a model, such as COSP, cannot either fully address this problem as not all ice components in the AGCMs are generally radiatively active. Future studies must continue to stress the need for a unified treatment of model ice water content output that is more inline with what is observed in nature. In doing so, model evaluation can better isolate problem areas. COSP also promises a more robust evaluation of clouds, since the definitions of clouds between models, as well as the various cloud-overlap assumptions add to the problems already described above.

Observations are critical to understanding and monitoring the climate system, and this thesis has relied on many observational sources. However, the current satellite platforms are no longer state of the art and some shortcomings of some current sensors will likely be addressed by the sensor's replacement. Therefore, it is important that future studies of tropics, consider new observational sources. Two examples of new datasets are:

1. EarthCARE, which is designed towards a better understanding of clouds, aerosols, and radiation interaction globally. This datasets will provide cloud, liquid water, ice, aerosol, and radiative heating profiles, as well as radiative flux observations at the top of the atmosphere. EarthCARE's dataset is created with climate models in mind and will improve upon the cloud ice profiles and provide cloud ice particle size information.
2. Global Precipitation Measurement (GPM), which is a network of satellites that will provide global measurements of rain and snow at 3-hourly intervals. The GPM mission focuses on Earth's water and energy cycles and is the successor to Tropical Rainfall Measuring Mission (TRMM), a dataset critical to this thesis. Over the tropics, MEGHA-TROPIQUES is a dedicated satellite for water cycle monitoring.

REFERENCES

- R. T. Austin, A. J. Heymsfield, and G. L. Stephens. Retrieval of ice cloud microphysical parameters using the CloudSat millimeter-wave radar and temperature. *J. Geophys. Res.*, 114(D8):D00A23, 2009. doi: 10.1029/2008JD010049.
- P. Bechtold, M. Köhler, T. Jung, F. Doblas-Reyes, M. Leutbecher, M. J. Rodwell, F. Vitart, and G. Balsamo. Advances in simulating atmospheric variability with the ECMWF model: From synoptic to decadal time-scales. *Q. J. R. Meteorol. Soc.*, 134(634):1337–1351, 2008. ISSN 1477-870X. doi: 10.1002/qj.289.
- V. Bjerknes, E. Volken, and S. Broennimann. The problem of weather prediction, considered from the viewpoints of mechanics and physics. *Meteorol. Z.*, 18:663–667, 1904. doi: 10.1127/0941-2948/2009/416.
- A. Bodas-Salcedo, M. J. Webb, S. Bony, H. Chepfer, J. L. Dufresne, S. A. Klein, Y. Zhang, R. Marchand, J. M. Haynes, R. Pincus, and V. O. John. COSP: satellite simulation software for model assessment. *Bull. Amer. Met. Soc.*, 92(8):1023–1043, 2011. doi: 10.1175/2011BAMS2856.1.
- S. Bony, R. Colman, V. M. Kattsov, R. P. Allan, C. S. Bretherton, J.-L. Dufresne, A. Hall, S. Hallegatte, M. M. Holland, W. Ingram, D. A. Randall, B. J. Soden, G. Tselioudis, and M. J. Webb. How well do we understand and evaluate climate change feedback processes? *J. Clim.*, 19(15):3445–3482, 2006. doi: 10.1175/JCLI3819.1.
- S. A. Buehler and V. O. John. A simple method to relate microwave radiances to upper tropospheric humidity. *J. Geophys. Res.*, 110(D2):D02110, 2005. doi: 10.1029/2004JD005111.
- S. A. Buehler, M. Kuvatov, V. O. John, M. Milz, B. J. Soden, D. L. Jackson, and J. Notholt. An upper tropospheric humidity data set from operational satellite microwave data. *J. Geophys. Res.*, 113, 2008. doi: 10.1029/2007JD009314.

- H. Chepfer, S. Bony, D. Winker, G. Cesana, J. L. Dufresne, P. Minnis, C. J. Stubenrauch, and S. Zeng. The GCM Oriented Calipso Cloud Product CALIPSO-GOCCP. *J. Geophys. Res.*, 115, 2010. doi: 10.1029/2009JD012251.
- E. J. Fetzer, W. G. Read, D. Waliser, B. H. Kahn, B. Tian, H. Vömel, F. W. Irion, H. Su, A. Eldering, M. T. Juarez, et al. Comparison of upper tropospheric water vapor observations from the Microwave Limb Sounder and Atmospheric Infrared Sounder. *J. Geophys. Res.*, 113(D22):D22110, 2008. doi: 10.1029/2008JD010000.
- P. R. Field and R. Wood. Precipitation and cloud structure in midlatitude cyclones. *J. Clim.*, 20(2):233–254, 2007. doi: 10.1175/JCLI3998.1.
- I. Folkins and R. V. Martin. The vertical structure of tropical convection and its impact on the budgets of water vapor and ozone. *J. Atmos. Sci.*, 62(5): 1560–1573, 2005. doi: 10.1175/JAS3407.1.
- R. M. Forbes. Microphysics: From intricacy to simplicity. In *Seminar on parametrization of subgrid physical processes, 1–4 September 2008*, pages 27–62, Shinfield Park, Reading, 2009. URL <http://www.ecmwf.int/publications>.
- A. Gettelman, W. D. Collins, E. J. Fetzer, A. Eldering, F. W. Irion, P. B. Duffy, and G. Bala. Climatology of upper-tropospheric relative humidity from the Atmospheric Infrared Sounder and implications for climate. *J. Clim.*, 19(23):6104–6121, 2006. ISSN 1520-0442. doi: 10.1175/JCLI3956.1.
- A. Gettelman, E. J. Fetzer, A. Eldering, and F. W. Irion. The global distribution of supersaturation in the upper troposphere from the Atmospheric Infrared Sounder. *J. Clim.*, 19(23):6089–6103, 2010. doi: 10.1175/JCLI3955.1.
- J. R. Holton. *An Introduction to Dynamic Meteorology*. Academic Press, 3 edition, 1994. ISBN 0-12-354355-X.
- G. Hong, G. Heygster, J. Miao, and K. Kunzi. Detection of tropical deep convective clouds from AMSU-B water vapor channels measurements. *J. Geophys. Res.*, 110(D9):D05205, 2005. doi: 10.1029/2004JD004949.
- G. J. Huffman, D. T. Bolvin, E. J. Nelkin, D. B. Wolff, R. F. Adler, G. Gu, Y. Hong, K. P. Bowman, and E. F. Stocker. The TRMM multisatellite precipitation analysis (TMPA): quasi-global, multiyear, combined-sensor precipitation estimates at fine scales. *J. Hydrometeorol.*, 8(1):38–55, 2007. doi: 10.1175/JHM560.1.

- C. D. Keeling. Climate change and carbon dioxide: An introduction. *Proceedings of the National Academy of Sciences*, 94(16):8273–8274, 1997. URL <http://www.pnas.org/content/94/16/8273.short>.
- J. T. Kiehl, J. J. Hack, G. B. Bonan, B. A. Boville, D. L. Williamson, and P. J. Rasch. The National Center for Atmospheric Research Community Climate Model: CCM3. *J. Clim.*, 11(6):1131–1149, 1998. doi: {10.1175/1520-0442(1998)011<1131:TNCFAR>2.0.CO;2}.
- D. B. Kirk-Davidoff, R. M. Goody, and J. G. Anderson. Analysis of sampling errors for climate monitoring satellites. *J. Clim.*, 18(6):810–822, 2005. doi: 10.1175/JCLI-3301.1.
- R. Knutti and G. C. Hegerl. The equilibrium sensitivity of the Earth’s temperature to radiation changes. *Nature Geoscience*, 1(11):735–743, 2008.
- C. Liu, E. J. Zipser, and S. W. Nesbitt. Global distribution of tropical deep convection: different perspectives from TRMM infrared and radar data. *J. Clim.*, 20(3):489–503, 2007. doi: 10.1175/JCLI4023.1.
- N. G. Loeb and S. Kato. Top-of-atmosphere direct radiative effect of aerosols over the tropical oceans from the Clouds and the Earth’s Radiant Energy System CERES satellite instrument. *J. Clim.*, 15(12):1474–1484, 2002. doi: 10.1175/1520-0442(2002)015<1474:TOADRE>2.0.CO;2.
- S. Manabe. Early development in the study of greenhouse warming: The emergence of climate models. *Ambio*, 26(1):47–51, 1997.
- S. Manabe and R. F. Strickler. Thermal equilibrium of the atmosphere with a convective adjustment. *J. Atmos. Sci.*, 21(4):361–385, 1964. doi: 10.1175/1520-0469(1964)021<0361:TEOTAW>2.0.CO;2.
- S. Manabe and R. T. Wetherald. Thermal equilibrium of the atmosphere with a given distribution of relative humidity. *J. Atmos. Sci.*, 24(3):241–259, 1967. doi: 10.1175/1520-0469(1967)024<0241:TEOTAW>2.0.CO;2.
- B. E. Mapes and R. A. Houze. Cloud clusters and superclusters over the oceanic warm pool. *Mon. Wea. Rev.*, 121(5):1398–1416, 1993. doi: 10.1175/1520-0493(1993)121<1398:CCASOT>2.0.CO;2.
- H. Masunaga. A satellite study of tropical moist convection and environmental variability: a moisture and thermal budget analysis. *J. Atmos. Sci.*, 70(8):2443–2466, 2013. doi: 10.1175/JAS-D-12-0273.1.

- K. McGuffie and A. Henderson-Sellers. *A Climate Modelling Primer*. John Wiley & Sons, Ltd, 3 edition, 2005. ISBN 0470857501.
- G. A. Meehl. Modeling the earth's climate. *Clim. Change*, 6:259–286, 1984. ISSN 0165-0009. doi: DOI:10.1007/BF00142476.
- G. Myhre, E. J. Highwood, K. P. Shine, and F. Stordal. New estimates of radiative forcing due to well mixed greenhouse gases. *Geophys. Res. Lett.*, 25(14):2715–2718, 1998. doi: 10.1029/98GL01908.
- D. Randall, M. Khairoutdinov, A. Arakawa, and W. Grabowski. Breaking the cloud parameterization deadlock. *Bull. Amer. Met. Soc.*, 84(11):1547–1564, 2003. doi: 10.1175/BAMS-84-11-1547.
- D. A. Randall, R. A. Wood, S. Bony, R. Colman, T. Fichefet, J. Fyfe, V. Kattsov, A. Pitman, J. Shukla, J. Srinivasan, R. J. Stouffer, A. Sumi, and K. E. Taylor. *Climate Models and Their Evaluation*. In: *Climate Change 2007: The Physical Science Basis. Contribution of Working Group I to the Fourth Assessment Report of the Intergovernmental Panel on Climate Change [Solomon, S. and Qin, D. and Manning, M. and Chen, Z. and Marquis, M. and Averyt, K. B. and Tignor, M. and H. L. Miller (eds.)]*. Cambridge University Press, Cambridge, United Kingdom and New York, NY, USA., 2007.
- W. G. Read, A. Lambert, J. Bacmeister, R. E. Cofield, L. E. Christensen, D. T. Cuddy, W. H. Daffer, B. J. Drouin, E. Fetzer, L. Froidevaux, R. Fuller, R. Herman, R. F. Jarnot, J. H. Jiang, Y. B. Jiang, K. Kelly, B. W. Knosp, L. J. Kovalenko, N. J. Livesey, H.-C. Liu, G. L. Manney, H. M. Pickett, H. C. Pumphrey, K. H. Rosenlof, X. Sabounchi, M. L. Santee, M. J. Schwartz, W. V. Snyder, P. C. Stek, H. Su, L. L. Takacs, R. P. Thurstans, H. Vömel, P. A. Wagner, J. W. Waters, C. R. Webster, E. M. Weinstock, and D. L. Wu. Aura Microwave Limb Sounder upper tropospheric and lower stratospheric H₂O and relative humidity with respect to ice validation. *J. Geophys. Res.*, 112:D24S35, 2007. doi: 10.1029/2007JD008752.
- R. Smith. *The Physics and Parameterization of Moist Atmospheric Convection*. Springer-Science+Business Media, B.V., 1997. ISBN 978-94-015-8828-7.
- B. J. Soden and R. Fu. A satellite analysis of deep convection, upper-tropospheric humidity, and the greenhouse effect. *J. Clim.*, 8(10):2333–2351, 1995. doi: 10.1175/1520-0442(1995)008<2333:ASAODC>2.0.CO;2.

- B. J. Soden and I. M. Held. An assessment of climate feedbacks in coupled ocean–atmosphere models. *J. Clim.*, 19(14):3354–3360, 2006. doi: 10.1175/JCLI3799.1.
- B. J. Soden, D. L. Jackson, V. Ramaswamy, M. D. Schwarzkopf, and X. Huang. The radiative signature of upper tropospheric moistening. *Science*, 310(5749):841–844, 2005. ISSN 0036-8075. doi: 10.1126/science.1115602.
- S. Solomon, D. Qin, M. Manning, Z. Chen, M. Marquis, K. B. Averyt, M. Tignor, and H. L. e. Miller. *Climate change 2007: The Physical science basis*. Cambridge University Press Cambridge, 2007. ISBN 0521880092.
- G. L. Stephens, D. G. Vane, R. J. Boain, G. G. Mace, K. Sassen, Z. Wang, A. J. Illingworth, E. J. O’Connor, W. B. Rossow, S. L. Durden, S. D. Miller, R. T. Austin, A. Benedetti, C. Mitrescu, and T. CloudSat Science Team. The CloudSat mission and the A-Train. *Bull. Amer. Met. Soc.*, 83(12):1771–1790, 2002. doi: 10.1175/BAMS-83-12-1771.
- W. Sun, G. Videen, S. Kato, B. Lin, C. Lukashin, and Y. Hu. A study of subvisual clouds and their radiation effect with a synergy of CERES, MODIS, CALIPSO, and AIRS data. *J. Geophys. Res. Atm.*, 116(D22):n/a–n/a, 2011. ISSN 2156-2202. doi: 10.1029/2011JD016422.
- H. Sundqvist. A parameterization scheme for non-convective condensation including prediction of cloud water content. *Q. J. R. Meteorol. Soc.*, 104(441):677–690, 1978. ISSN 1477-870X. doi: 10.1002/qj.49710444110.
- J. Thuburn. Some basic dynamics relevant to the design of atmospheric model dynamical cores. In P. Lauritzen, C. Jablonowski, M. Taylor, and R. Nair, editors, *Numerical Techniques for Global Atmospheric Models*, volume 80 of *Lecture Notes in Computational Science and Engineering*, pages 3–27. Springer Berlin Heidelberg, 2011. ISBN 978-3-642-11639-1. doi: 10.1007/978-3-642-11640-7_1. URL http://dx.doi.org/10.1007/978-3-642-11640-7_1.
- H. Tost, P. Jöckel, and J. Lelieveld. Influence of different convection parameterisations in a GCM. *Atmos. Chem. Phys.*, 6(12):5475–5493, 2006. doi: 10.5194/acp-6-5475-2006.
- D. M. Winker, W. H. Hunt, and M. J. McGill. Initial performance assessment of CALIOP. *Geophys. Res. Lett.*, 34(19):L19803, 2007. doi: 10.1029/2007GL030135.

-
- M. D. Zelinka and D. L. Hartmann. Response of humidity and clouds to tropical deep convection. *J. Clim.*, 22(9):2389–2404, 2009. doi: 10.1175/2008JCLI2452.1.

